

A new species of *Nanhsiungchelys* (Testudines: Cryptodira: Nanhsiungchelyidae) from the Upper Cretaceous of Nanxiong Basin, China

Yuzheng Ke^{Corresp., 1}, Imran A Rahman^{2,3}, Hanchen Song¹, Jinfeng Hu¹, Kecheng Niu^{4,5}, Fasheng Lou⁶, Hongwei Li⁷, Fenglu Han^{Corresp., 1}

¹ School of Earth Science, China University of Geosciences (Wuhan), Wuhan, Hubei, People's Republic of China

² The Natural History Museum, London, United Kingdom

³ Oxford University Museum of Natural History, Oxford, United Kingdom

⁴ State Key Laboratory of Cellular Stress Biology, School of Life Sciences, Xiamen University, Xiamen, Fujian, People's Republic of China

⁵ Yingliang Stone Natural History Museum, Nan'an, Fujian, People's Republic of China

⁶ Jiangxi Geological Survey and Exploration Institute, Nanchang, Jiangxi, People's Republic of China

⁷ Guangdong Geological Survey Institute, Guangzhou, Guangdong, People's Republic of China

Corresponding Authors: Yuzheng Ke, Fenglu Han
Email address: key1480@163.com, hanfl@cug.edu.cn

Nanhsiungchelyidae are a group of large turtles that lived in Asia and North America during the Cretaceous. Here we report a new species of nanhsiungchelyid, *Nanhsiungchelys yangi* sp. nov., from the Upper Cretaceous of Nanxiong Basin, China. The specimen consists of a well-preserved skull and lower jaw, as well as the anterior parts of the carapace and plastron. The diagnostic features of *Nanhsiungchelys* include a large entire carapace length (~55.5 cm), a network of sculptures consisting of pits and ridges on the surface of the skull and shell, shallow cheek emargination and temporal emargination, deep nuchal emargination, and a pair of anterolateral processes on the carapace. However, *Nanhsiungchelys yangi* differs from the other species of *Nanhsiungchelys* mainly in having a triangular-shaped snout (in dorsal view) and wide anterolateral processes on the carapace. Additionally, some other characteristics (e.g., the premaxilla is higher than wide, the maxilla is unseen in dorsal views, a small portion of the maxilla extends posterior and ventral of the orbit, and the parietal is bigger than the frontal) are strong evidence to distinguish *Nanhsiungchelys yangi* from *Nanhsiungchelys wuchinensis*. A phylogenetic analysis of nanhsiungchelyids places *Nanhsiungchelys yangi* and *Nanhsiungchelys wuchingensis* as sister taxa. *Nanhsiungchelys yangi* and some other nanhsiungchelyids bear distinct anterolateral processes on the carapace, which have not been reported in any extant turtles and may have played a role in protecting the head. The Nanxiong Basin was extremely hot during the Late Cretaceous, and so we suggest that nanhsiungchelyids might have immersed themselves in mud or water to avoid the hot weather, similar to

some extant tortoises. If they were capable of swimming, our computer simulations of fluid flow suggest the anterolateral processes could have reduced drag during locomotion.

1
2 **A new species of *Nanhsiungchelys* (Testudines:**
3 **Cryptodira: Nanhsiungchelyidae) from the Upper**
4 **Cretaceous of Nanxiong Basin, China**

5
6
7 Yuzheng Ke¹, Imran A. Rahman^{2,3}, Hanchen Song¹, Jinfeng Hu¹, Kecheng Niu^{4,5}, Fasheng
8 Lou⁶, Hongwei Li⁷, Fenglu Han¹

9 ¹ School of Earth Science, China University of Geosciences (Wuhan), Wuhan, Hubei, China.

10 ² The Natural History Museum, London, UK.

11 ³ Oxford University Museum of Natural History, Oxford, UK.

12 ⁴ State Key Laboratory of Cellular Stress Biology, School of Life Sciences, Xiamen University,
13 Xiamen, Fujian, China

14 ⁵ Yingliang Stone Natural History Museum, Nan'an, Fujian, China

15 ⁶ Jiangxi Geological Survey and Exploration Institute, Nanchang, Jiangxi, China

16 ⁷ Guangdong Geological Survey Institute, Guangzhou, Guangdong, China

17
18 Corresponding Author:

19 Fenglu Han

20 Lumo Road, Wuhan, Hubei, 430074, China

21 Email address: hanfl@cug.edu.cn

22 Yuzheng Ke

23 Lumo Road, Wuhan, Hubei, 430074, China

24 Email address: key1480@163.com

25
26 **Abstract**

27 Nanhsiungchelyidae are a group of large turtles that lived in Asia and North America during the
28 Cretaceous. Here we report a new species of nanhsiungchelyid, *Nanhsiungchelys yangi* sp. nov.,
29 from the Upper Cretaceous of Nanxiong Basin, China. The specimen consists of a well-
30 preserved skull and lower jaw, as well as the anterior parts of the carapace and plastron. The
31 diagnostic features of *Nanhsiungchelys* include a large entire carapace length (~55.5 cm), a
32 network of sculptures consisting of pits and ridges on the surface of the skull and shell, shallow
33 cheek emargination and temporal emargination, deep nuchal emargination, and a pair of
34 anterolateral processes on the carapace. However, *Nanhsiungchelys yangi* differs from the other
35 species of *Nanhsiungchelys* mainly in having a triangular-shaped snout (in dorsal view) and wide
36 anterolateral processes on the carapace. Additionally, some other characteristics (e.g., the
37 premaxilla is higher than wide, the maxilla is unseen in dorsal views, a small portion of the
38 maxilla extends posterior and ventral of the orbit, and the parietal is bigger than the frontal) are

39 strong evidence to distinguish *Nanhsiungchelys yangi* from *Nanhsiungchelys wuchingensis*. A
40 phylogenetic analysis of nanhsiungchelyids places *Nanhsiungchelys yangi* and *Nanhsiungchelys*
41 *wuchingensis* as sister taxa. *Nanhsiungchelys yangi* and some other nanhsiungchelyids bear
42 distinct anterolateral processes on the carapace, which have not been reported in any extant
43 turtles and may have played a role in protecting the head. The Nanxiong Basin was extremely
44 hot during the Late Cretaceous, and so we suggest that nanhsiungchelyids might have immersed
45 themselves in mud or water to avoid the hot weather, similar to some extant tortoises. If they
46 were capable of swimming, our computer simulations of fluid flow suggest the anterolateral
47 processes could have reduced drag during locomotion.

48

49 Introduction

50 Nanhsiungchelyidae are an extinct group of Pan-Trionychia, which lived in Asia and North
51 America from the Early Cretaceous until their extinction at the Cretaceous–Paleogene boundary
52 (Hirayama *et al.*, 2000; Li & Tong, 2017; Joyce *et al.*, 2021). These turtles are characterized by a
53 large body size (maximum carapace length of about 120 cm as preserved), flat carapace relative
54 to tortoises, stubby elephantine limbs, and shells covered with a network of sculptures consisting
55 of pits and ridges (Yeh, 1966; Hutchison & Archibald, 1986; Brinkman *et al.*, 2015; Hu *et al.*,
56 2016; Li & Tong, 2017). In addition, these turtles produced thick-shelled (~1.8 mm) eggs and are
57 thought to have had similar reproductive strategies to extant tortoises (e.g., large and spherical
58 eggs) (Ke *et al.*, 2021). Recently, the morphology and phylogenetic relationships of
59 nanhsiungchelyids have been studied in detail (Danilov *et al.*, 2013; Brinkman *et al.*, 2015; Tong
60 *et al.*, 2016; Mallon & Brinkman, 2018; Tong & Li, 2019). Among the eight genera of
61 Nanhsiungchelyidae, most taxa typically have a relatively short carapace, shallow nuchal
62 emargination, narrow neurals and vertebral scutes, and lack large anterior processes on the
63 carapace (Tong & Li, 2019). In contrast, *Nanhsiungchelys* and *Anomalocheilus* (which form a
64 sister group) share an elongated shell, a wide and deep nuchal emargination, large anterior
65 process on the carapace, wide neurals and vertebral scutes, and a sub-triangular first vertebral
66 scute with a very narrow anterior end (Tong & Li, 2019). These two genera have only been found
67 in southern China and Japan (Hirayama *et al.*, 2001; Hirayama *et al.*, 2009; Li & Tong, 2017;
68 Tong & Li, 2019), whereas other nanhsiungchelyids have a wider geographical distribution
69 (Danilov & Syromyatnikova, 2008; Mallon & Brinkman, 2018).

70 *Nanhsiungchelys* and *Anomalocheilus* are unique among Mesozoic turtles in possessing distinct
71 anterolateral processes on the carapace, with a similar body structure known in the Miocene side-
72 necked turtle *Stupendemys geographicus* (Cadena *et al.*, 2020). Palaeontologists have debated
73 whether nanhsiungchelyids were aquatic or terrestrial for nearly 60 years (see Mallon &
74 Brinkman (2018) for a detailed overview), but the ecological role of the anterolateral processes
75 has largely been ignored. It was previously suggested they played a role in protecting the head
76 (Hirayama *et al.*, 2001) or facilitating sexual displays (Hirayama & Sonoda, 2012), but further
77 study of their function is required.

78 In China, six species of nanhsiungchelyids have been reported (Table 1), with many
79 specimens recovered from the Upper Cretaceous of Nanxiong Basin, Guangdong Province. *Yeh*
80 (1966) described the first species, *Nanhsiungchelys wuchingensis*, which was restudied by *Tong*
81 & *Li* (2019). *Hirayama et al.* (2009) provided a preliminary study of a large Cretaceous turtle
82 (SNHM 1558) which they placed within Nanhsiungchelyidae; *Li & Tong* (2017) later attributed
83 this to *Nanhsiungchelys*. In addition, two eggs (IVPP V2789) from Nanxiong Basin were
84 assigned to nanhsiungchelyids based on their co-occurrence with *Nanhsiungchelys wuchingensis*
85 (*Young, 1965*).

86 Nanxiong Basin (Fig. 1A) is a NE-trending faulted basin controlled by the Nanxiong Fault in
87 the northern margin, covering an area of about 1800 km² and spanning Guangdong and Jiangxi
88 provinces in China (*Zhang et al., 2013*). Well-exposed outcrops of Cretaceous–Paleogene strata
89 occur in Nanxiong Basin (*Ling et al., 2005*), and the lithostratigraphy of the Upper Cretaceous in
90 this region has been studied extensively (see *Zhang et al. (2013)* for details). In 1966, the
91 holotype of *Nanhsiungchelys wuchingensis* (IVPP V3106) was recovered from Nanxiong Basin,
92 with the stratum where the fossil was found named the Nanxiong Group (*Yeh 1966*).
93 Subsequently, *Zhao et al. (1991)* split Nanxiong Group into the upper Pingling Formation and
94 lower Yuanpu Formation, reporting two K–Ar ages for the Yuanpu Formation (67.04±2.31 Ma
95 and 67.37±1.49 Ma). *Zhang et al. (2013)* further divided the original Yuanpu Formation into the
96 Jiangtou, Yuanpu, Dafeng, and Zhutian formations, with the new Yuanpu Formation just a small
97 part of the original Yuanpu Formation. Most recently, the Yuanpu Formation was eliminated
98 entirely, and the Nanxiong Group now consists of Dafeng, Zhutian, and Zhenshui formations
99 (*Guangdong Geological Survey Institute, 2017*). This terminology was also used by *Xi et al.*
100 (2021), who summarized lithostratigraphic subdivision and correlation for the Cretaceous of
101 China. According to this scheme, the holotypes of *Nanhsiungchelys wuchingensis* (IVPP V3106)
102 and *N. yangi* (CUGW VH108, see below) both come from the Dafeng Formation.

103 The Dafeng Formation comprises purple-red, brick-red, and brownish-red conglomerate,
104 sandy conglomerate, and gravel-bearing sandstone, and is intercalated with sandstone, siltstone
105 and silty mudstone (*Guangdong Geological Survey Institute, 2017*). It ranges in age from the
106 Cenomanian to the middle Campanian (*Xi et al., 2021*). In addition to *Nanhsiungchelys*, many
107 vertebrate fossils have been recovered from the Dafeng Formation, including: the dinosaur
108 *Nanshiungosaurus brevispinus* (*Zanno, 2010*); the turtle eggs *Oolithes nanhsiungensis* (*Young,*
109 *1965*); and the dinosaur eggs *Macroolithus rugustus*, *Nanhsiungoolithus chuetienensis*,
110 *Ovaloolithus shitangensis*, *O. nanxiongensis*, and *Shixingoolithus erbeni* (*Zhao et al., 2015*).

111 Here, we report a new species of *Nanhsiungchelys* from Nanxiong Basin based on a complete
112 skull and partial postcranial skeleton. This allows us to investigate the taxonomy and
113 morphology of nanhsiungchelyids, and based on this we carry out a phylogenetic analysis of the
114 group. In addition, we discuss potential functions of the large anterolateral processes (using
115 computational fluid dynamics to test a possible role in drag reduction) and consider the
116 implications for the ecology of this taxon.

117

118 **Materials & Methods**

119 **Fossil specimen.** The specimen (CUGW VH108) consists of a well-preserved skull and lower
120 jaw, together with the anterior parts of the carapace and plastron (Figs. 2–4). This specimen was
121 collected by a local farmer from southeast of Nanxiong Basin, near the Zhenjiang River. Based
122 on the brownish-red siltstone near the skeleton, it was most likely from the Dafeng Formation
123 (*Guangdong Geological Survey Institute, 2017*). CUGW VH108 is housed in the paleontological
124 collections of China University of Geosciences (Wuhan). The skeleton was prepared using an
125 Engraving Pen AT-310 and was photographed with a Canon EOS 6D camera.

126 **Nomenclatural acts.** The electronic version of this article in Portable Document Format (PDF)
127 will represent a published work according to the International Commission on Zoological
128 Nomenclature (ICZN), and hence the new names contained in the electronic version are
129 effectively published under that Code from the electronic edition alone. This published work and
130 the nomenclatural acts it contains have been registered in ZooBank, the online registration
131 system for the ICZN. The ZooBank LSIDs (Life Science Identifiers) can be resolved and the
132 associated information viewed through any standard web browser by appending the LSID to the
133 prefix <http://zoobank.org/>. The LSID for this publication is:
134 urn:lsid:zoobank.org:pub:F53B5FA5-D018-453D-814D-C854810EFEFE. The online version of
135 this work is archived and available from the following digital repositories: PeerJ, PubMed
136 Central SCIE and CLOCKSS.

137 **Phylogenetic analysis.** Parsimony phylogenetic analysis was performed using the software TNT
138 1.5 (*Goloboff & Catalano, 2016*). The data matrix used herein was updated from *Tong & Li*
139 (*2019*) and *Mallon & Brinkman (2018)*, and includes 17 taxa and 50 characters. *Adocus* was set
140 as the outgroup following *Tong & Li (2019)*. Because there are five inframarginal scutes on
141 *Jiangxichelys ganzhouensis* (*Tong et al., 2016*), character 37 was modified to: “Inframarginals:
142 (0) five to three pairs; (1) two pairs; (2) absent”. In addition, on the basis of *Tong et al. (2016)*,
143 character 48 was changed in *Jiangxichelys ganzhouensis* from ? to 1 (i.e., ratio of midline
144 epiplastral suture length to total midline plastral length greater than 0.1). The length to width
145 ratios of the carapace of *Nanhsiungchelys* and *Anomalochelys* are equal to or larger than 1.6
146 (*Hirayama et al., 2001; Hirayama et al., 2009; Tong & Li, 2019*), whereas the other genera (e.g.,
147 *Basilemys*) exhibit smaller ratios (*Mallon & Brinkman, 2018*). An example with a ratio between
148 1.4 and 1.6 has not been found in any nanhsiungchelyids yet. Therefore, a new character was
149 added: “Length to width ratio of the carapace: (0) less than 1.4; (1) equal to or larger than 1.6”.
150 Moreover, *Yuchelys nanyangensis* was added to the data matrix based on *Tong et al. (2012)*. A
151 total of 13 characters out of 50 could be coded for *Nanhsiungchelys yangi*, representing only
152 26% of the total number of characters. This is because the new species is based on a partial
153 specimen missing many of the features scored in other taxa. The analysis was conducted using a
154 traditional search with 1000 replicates. A tree bisection reconnection (TBR) swapping algorithm
155 was employed, and 10 trees were saved per replicate. All characters were treated as unordered
156 and of equal weight. Standard bootstrap support values were calculated using a traditional search
157 with 100 replicates. Bremer support values were also calculated (*Bremer, 1994*). In addition, a

158 time-scaled phylogeny was generated in R (<https://www.r-project.org/>) using our strict consensus
159 tree and the first / last appearance datum (FAD / LAD) of all taxa. The R package Strap (*Bell &*
160 *Lloyd, 2014*) was used to estimate divergence times and the function geoscalePhylo was used to
161 plot the time-scaled tree against a geological timescale.

162 **Computational fluid dynamics.** Computational fluid dynamics (CFD) simulations of water
163 flow were performed in the software COMSOL Multiphysics (v. 5.6). Three-dimensional digital
164 models of *Nanhsiungchelys yangi* and two ‘hypothetical turtles’ without anterolateral processes
165 were created using COMSOL’s in-built geometry tools. These models were placed in cylindrical
166 flow domains, with the material properties of water assigned to the space surrounding the models
167 and the swimming speeds of the extant large turtle used as flow velocities at the inlet. CFD
168 simulations were performed using a stationary solver, and based on the results drag forces were
169 extracted for each model. The main steps including the construction of digital models,
170 specification of fluid properties and boundary conditions, meshing, and computation are detailed
171 in Supplemental Information 3.

172 **Institutional abbreviations.** CUGW, China University of Geosciences (Wuhan), Wuhan, China;
173 HGM, Henan Geological Museum, Zhengzhou, China; IMM, Inner Mongolia Museum, Huhhot,
174 China; IVPP, Institute of Vertebrate Paleontology and Paleoanthropology, Chinese Academy of
175 Sciences, Beijing, China; LJU, Lanzhou Jiaotong University, Lanzhou, China; NHMG, Natural
176 History Museum of Guangxi, Nanning, China; NMBY, Nei Mongo Bowuguan, Huhhot, China;
177 SNHM, Shanghai Natural History Museum, Shanghai, China; UB, University of Bristol, Bristol,
178 UK; UPC, China University of Petroleum (East China), Qingdao, China; YSNHM, Yingliang
179 Stone Natural History Museum, Nan’an, China.

180

181 **Results**

182 **Systematic paleontology**

183 Testudines Linnaeus, 1758

184 Cryptodira Cope, 1868

185 Nanhsiungchelyidae Yeh, 1966

186 *Nanhsiungchelys* Yeh, 1966

187 **Emended diagnosis.** A genus of Nanhsiungchelyidae of medium-large size, with an entire
188 carapace length of 0.5–1.1 m. The surface of the skull, lower jaw, and both carapace and plastron
189 are covered with sculpturing consisting of large pits formed by a network of ridges. Temporal
190 emargination and cheek emargination are shallow; orbits located at about mid-length of the skull
191 and facing laterally; jugal forms the lower margin of the orbit. Carapace elongate, with a deep
192 nuchal emargination and a pair of large anterolateral processes that extend forward and are
193 formed entirely by the first peripheral; wide neural plates and vertebral scutes; gulars fused and
194 extend deeply onto the entoplastron; extragulars absent; complete row of narrow inframarginals.
195 Wide angle between the acromion process and scapula process of about 105°. One large dermal
196 plate located above the manus.

197 **Type species.** *Nanhsiungchelys wuchingensis* Yeh, 1966

198 **Distribution.** Guangdong, China

199

200 *Nanhsiungchelys yangi* sp. nov.

201 **Etymology.** The species epithet *yangi* is in memory of paleontologist Zhongjian Yang (Chung-
202 Chien Young).

203 **Holotype.** CUGW VH108, a partial skeleton comprising a well-preserved skull and lower jaw
204 and the anterior parts of the carapace and plastron (Figs. 2–4).

205 **Locality and horizon.** Nanxiong, Guangdong, China. Dafeng Formation, Upper Cretaceous,
206 Cenomanian to middle Campanian (*Xi et al., 2021*).

207 **Diagnosis.** A medium-sized species of *Nanhsiungchelys* with an estimated entire carapace length
208 of more than 0.5 meters. It differs from *Nanhsiungchelys wuchingensis* in the following
209 combination of characters: snout is triangular in dorsal view; premaxilla greater in height than
210 length; posteroventral ramus of the maxilla extends to the ventral region of the orbit; the dorsal
211 margin of the maxilla is relatively straight; jugal is greater in height than width; prefrontal is
212 convex dorsally behind the apertura narium externa; temporal emargination is mainly formed by
213 the parietal; paired parietals are bigger than the frontals in dorsal view; middle and posterior
214 parts of the mandible are more robust than the most anterior part in ventral view; anterolateral
215 processes is wide; and the angle between the two anterior edges of the entoplastron is wide
216 (~110°).

217 **Description.**

218 **General aspects of the skull.** The skull is large, with a length of 13 cm (Fig. 3A, B). It is well
219 preserved, but numerous cracks on its outer surface limit the identification of bone sutures. The
220 snout (i.e., the parts anterior to the orbit) is large, equal to about 1/3 the length of the skull, and
221 longer than in *Jiangxichelys neimongolensis* and *Zangerlia ukhaachelys* (*Joyce & Norell, 2005*;
222 *Brinkman et al., 2015*). In dorsal view, the snout is close to triangular in outline with a narrow
223 anterior end (Fig. 3A, B). In lateral views, the robust snout is nearly as deep as the whole skull,
224 with the anterior end roughly perpendicular to the horizon (Fig. 3C–F). These features differ
225 from *Nanhsiungchelys wuchingensis* in which the snout is flattened, with the anterior end
226 increasing in width in dorsal view (*Tong & Li, 2019*), giving it a trumpet shape. A large apertura
227 narium externa is located in the front part of the snout, which is roughly lozenge shaped and
228 greater in height than width in anterior view (Fig. 2). Because the posterior part of the skull is not
229 preserved, it is difficult to accurately determine the morphological characteristics of cheek
230 emargination (Fig. 3C–F). Nevertheless, based on the visible bone morphology, we infer that the
231 cheek emargination was absent or low, rather than deep (i.e., to the level or even beyond the
232 level of orbit, see e.g., *Emydura macquarrii*) (*Li & Tong, 2017*). Posteriorly, the temporal
233 emargination is weakly developed (Fig. 3A, B), which is similar to *Nanhsiungchelys*
234 *wuchingensis* (*Tong & Li, 2019*) and the ‘Hefei specimen’ (*Hu et al., 2016*), but differs from
235 *Jiangxichelys neimongolensis*, *J. ganzhouensis* and *Zangerlia ukhaachelys* (*Brinkman & Peng,*
236 *1996; Joyce & Norell, 2005; Tong et al., 2016*). The surface of the skull (as well as those of the

237 carapace and plastron) is covered with a network of sculptures consisting of pits and ridges,
238 which is one of the synapomorphies of *Nanhsiungchelyidae* (Li & Tong, 2017).

239 **Premaxilla.** A small bone in the anterior and ventral part of the maxilla is identified as the
240 premaxilla (Fig. 3C–F). It is greater in height than width, similar to *Jiangxichelys*
241 *neimongolensis* and *Zangerlia ukhaachelys* (Joyce & Norell, 2005; Brinkman et al., 2015), but
242 differs from *Nanhsiungchelys wuchingensis* in which the premaxilla is wider than it is high in
243 lateral view and has an inverse Y-shape in ventral view (Tong & Li, 2019). Given the existence
244 of the large lozenge-shaped external narial opening, the contact between the left and right
245 premaxillae may be short, unlike the condition of *Jiangxichelys neimongolensis* (Brinkman et al.,
246 2015). However, the poor preservation of elements near the external narial opening prevents
247 more detailed observations, and the possibility of a Y-shaped premaxilla as in *Nanhsiungchelys*
248 *wuchingensis* cannot be excluded.

249 **Maxilla.** The maxilla is large and trapezoidal in outline (Fig. 3C–F). The main body is located
250 anterior to the orbit, but the posteroventral ramus extends to the ventral region of the orbit, which
251 differs from the situation in *Nanhsiungchelys wuchingensis*, in which the maxilla is located
252 entirely anterior to the orbit (Tong & Li, 2019), and also differs from that in most other turtles
253 (including *Zangerlia ukhaachelys* and *Jiangxichelys neimongolensis*), in which the maxilla
254 contributes to the lower rim of the orbit (Joyce & Norell, 2005; Brinkman et al., 2015). In lateral
255 view, the dorsal margin of the maxilla is relatively straight and extends posteriorly to the mid-
256 region of the eye socket, which is similar to the condition in some extant turtles (e.g.,
257 *Platysternon megacephalum*) (Li & Tong, 2017). However, this differs from the condition in
258 *Nanhsiungchelys wuchingensis* in which the top of the maxilla is curved dorsally (Tong & Li,
259 2019), and also differs from *Zangerlia ukhaachelys* and *Jiangxichelys neimongolensis* in which
260 the top of the maxilla tapers anterodorsally (Joyce & Norell, 2005; Brinkman et al., 2015).

261 **Jugal.** The jugal is shaped like a parallelogram in lateral view (Fig. 3C–F). It is greater in height
262 than width, unlike *Nanhsiungchelys wuchingensis*, in which the jugal is wider than it is high
263 (Tong & Li, 2019). The jugal consists of the lower rim of the orbit, which is similar to that of
264 *Nanhsiungchelys wuchingensis*, but differs from most turtles, in which this structure is mainly
265 formed by the maxilla (Tong & Li, 2019). The jugal of *Nanhsiungchelys yangi* also differs from
266 that of *Jiangxichelys ganzhouensis*, in which the jugal is more posteriorly located (Tong et al.,
267 2016). The jugal contacts with the maxilla anteriorly, and this suture is sloped. The terminal parts
268 of the jugal contacts with the quadratojugal.

269 **Quadratojugal.** The bone that is posterior to the jugal and ventral to the postorbital is identified
270 as the quadratojugal (Fig. 3C–F). Its location is similar in *Nanhsiungchelys wuchingensis* (Tong
271 & Li, 2019), but the full shape is uncertain due to covering by the carapace.

272 **Prefrontal.** In dorsal view, each prefrontal is large and elongate anteroposteriorly, and narrows
273 anteriorly and enlarges posteriorly (Fig. 3A, B). The portion in front of the orbit is entirely
274 composed of the prefrontal (Fig. 3A, B), which differs from *Nanhsiungchelys wuchingensis* in
275 which the maxilla extends dorsally to the prefrontal and occupies some space (Tong & Li, 2019).
276 The paired prefrontals contact each other at the midline and form an approximate arrow shape.

277 They form the dorsal margin of apertura narium externa anteriorly, the anterodorsal rim of the
278 orbit posterolaterally, and contact the frontal and postorbital posteriorly (Fig. 3A, B). The contact
279 area between the prefrontal and frontal is convex anteriorly (i.e., ‘Λ’-shaped), which is similar to
280 that seen in *Nanhsiungchelys wuchingensis* (Tong & Li, 2019). In lateral view, the prefrontal is
281 anterior to the postorbital and dorsal to the maxilla, and consists of the anterodorsal rims of the
282 orbit (Fig. 3C–F). This is similar to the anatomy in *Nanhsiungchelys wuchingensis*, *Jiangxichelys*
283 *neimongolensis* and *Zangerlia ukhaachelys* (Brinkman & Peng, 1996; Joyce & Norell, 2005;
284 Tong & Li, 2019). Behind the apertura narium externa, the prefrontal is convex dorsally (Fig.
285 3C–F), rather than concave as in *Nanhsiungchelys wuchingensis* (Tong & Li, 2019).

286 **Frontal.** The paired frontals form a large pentagon that is located in the center of the skull roof
287 (Fig. 3A, B), which is similar to the condition in *Nanhsiungchelys wuchingensis* and *Zangerlia*
288 *ukhaachelys* (Joyce & Norell, 2005; Tong & Li, 2019). In these taxa, the anterior margins
289 constitute a “Λ” shape for articulating with the prefrontal. The lateral and posterior margins
290 contact the postorbital and parietal, respectively. The frontal is excluded from the rim of the
291 orbit, as in *Nanhsiungchelys wuchingensis* and *Zangerlia ukhaachelys* (Joyce & Norell, 2005;
292 Tong & Li, 2019). Notably, a line between the paired frontals (Fig. 3A, B) might be a suture or
293 crack. We think it most likely represents a suture because a similar structure appears in other
294 nanhsiungchelyid specimens (Joyce & Norell, 2005; Tong & Li, 2019). Interestingly, this suture
295 is unusually slanted, which may be the result of developmental abnormality and needs more
296 specimens for verification.

297 **Postorbital.** The postorbital is subtriangular in outline and elongated anteroposteriorly, and it
298 composes part of the lateral skull roof. Most parts of the postorbital are behind the orbit, but the
299 anterodorsal process extends to the dorsal edge of the orbit (Fig. 3C–F). Thus, the postorbital
300 consists of the posterior-upper and posterior rims of the orbits, which is similar to the elements
301 of *Nanhsiungchelys wuchingensis*, *Jiangxichelys ganzhouensis* and *Zangerlia ukhaachelys*
302 (Joyce & Norell, 2005; Tong et al., 2016; Tong & Li, 2019). The postorbital contacts the
303 prefrontal and frontal anteriorly, the jugal and quadratojugal ventrally, and the parietal medially
304 (Fig. 3A–F). In dorsal view, the shape of the posterior margin of the postorbital is uncertain due
305 to its poor preservation and because it is partly obscured by the carapace. It is also uncertain if
306 the postorbital constitutes the rim of temporal emargination. Notably, the postorbital in both
307 *Nanhsiungchelys yangi* and *N. wuchingensis* is relatively large in size (Tong & Li, 2019),
308 whereas just a small element forms the ‘postorbital bar’ in *Jiangxichelys ganzhouensis* and
309 *Zangerlia ukhaachelys* (Joyce & Norell, 2005; Tong et al., 2016).

310 **Parietal.** The trapezoidal parietal contributes to the posterior part of the skull roof (Fig. 3A, B),
311 which is similar to the condition in *Nanhsiungchelys wuchingensis* (Tong & Li, 2019). However,
312 the paired parietals are bigger than the frontals in dorsal view, contrasting with the configuration
313 in *Nanhsiungchelys wuchingensis* (Tong & Li, 2019). The parietal contacts the frontal anteriorly
314 and the postorbital laterally, and these boundaries are not straight. Posteriorly, the parietal
315 contributes to the upper temporal emarginations, but the absence of the posterior ends of the

316 parietal (especially the right part) hampers the identification of the rims of upper temporal
317 emarginations.

318 **Mandible.** The mandible is preserved in situ and tightly closed with the skull (Fig. 3C–F). The
319 location of the mandible is posterior and interior to the maxillae (Fig. 4). As a result, the beak is
320 hidden, but the lower parts of the mandible can be observed. The symphysis is fused, which is
321 similar to the mandible of *Nanhsiungchelys wuchingensis* (Tong & Li, 2019). In ventral view, the
322 most anterior part of the mandible appears slender, but the middle and posterior parts are robust
323 (Fig. 4). This differs from *Nanhsiungchelys wuchingensis*, in which nearly all parts of the
324 mandible are equal in width (Tong & Li, 2019).

325 **Carapace.** Only the anterior parts of the carapace are preserved (Fig. 3A, B). The preserved
326 parts indicate a deep nuchal emargination and a pair of anterolateral processes, which are similar
327 to those of *Anomalochelys angulata*, *Nanhsiungchelys wuchingensis*, *Nanhsiungchelys* sp.
328 (SNHM 1558), and the ‘Hefei specimen’ (Hirayama et al., 2001; Hirayama et al., 2009; Hu et
329 al., 2016; Tong & Li, 2019). In contrast, the carapaces of other genera of nanhsiungchelyids
330 (including *Basilemys*, *Hanbogdemys*, *Kharakhutulia*, *Jiangxichelys* and *Zangerlia*) usually have
331 a shallow nuchal emargination and/or lack the distinctive anterolateral processes (Mlynarski,
332 1972; Sukhanov, 2000; Sukhanov et al., 2008; Tong & Mo, 2010; Danilov et al., 2013; Mallon &
333 Brinkman, 2018). In dorsal view, each anterolateral process of *Nanhsiungchelys yangi* is very
334 wide (nearly 90°), similar to *Nanhsiungchelys wuchingensis* (Tong & Li, 2019); however, the
335 anterolateral processes of *Anomalochelys angulata* and *Nanhsiungchelys* sp. (SNHM 1558) are
336 slender crescent-shaped and horn-shaped, respectively, both of which are sharper than in
337 *Nanhsiungchelys yangi* (Hirayama et al., 2001; Hirayama et al., 2009). Among the above
338 species of *Nanhsiungchelys* and *Anomalochelys*, there is always a distinct protrusion at the tip of
339 each anterolateral process, and this protrusion becomes more prominent in *Anomalochelys*
340 *angulata* (Fig. 5B) and *Nanhsiungchelys* sp. (SNHM 1558) (Hirayama et al., 2001; Hirayama et
341 al., 2009). In *Nanhsiungchelys wuchingensis* and *Anomalochelys angulata* the most anterior end
342 of the process shows varying degrees of bifurcation (Fig. 5B) (Hirayama et al., 2001; Tong & Li,
343 2019), but this bifurcation does not occur in *Nanhsiungchelys yangi* and *Nanhsiungchelys* sp.
344 (SNHM 1558) (Hirayama et al., 2009). Due to the lack of sutures preserved on the surface of the
345 carapace, it is difficult to determine whether these processes are composed of nuchal or
346 peripheral plates. However, considering the similarity in shape of the anterolateral processes in
347 *Nanhsiungchelys yangi* and *N. wuchingensis*, the anterolateral processes of *N. yangi* may be
348 formed by the first peripheral plates (as in *N. wuchingensis*).

349 **Plastron.** A large plate under the mandible is identified as the anterior part of the plastron (Fig.
350 4). The anterior edge of the eiplastron extends anteriorly beyond the deepest part of nuchal
351 emargination (Fig. 4), similar to that seen in *Basilemys*, *Hanbogdemys*, *Jiangxichelys*,
352 *Nanhsiungchelys*, and *Zangerlia* (Sukhanov, 2000; Danilov et al., 2013; Brinkman et al., 2015;
353 Tong et al., 2016; Mallon & Brinkman, 2018; Tong & Li, 2019). The anterior part of the
354 eiplastron is very thin, but it increases in thickness posteriorly and laterally (Fig. 2). Although
355 poorly preserved, the angle between the left and right edges can be measured as about 55°, which

356 is wider than *Hanbogdemys orientalis* (Sukhanov, 2000). The epiplastra are paired and connected
357 at the midline. Because only the anterior part of the entoplastron is preserved, it is hard to discern
358 its shape. The anterior edges of the entoplastron are strongly convex, and lead into the posterior
359 part of the epiplastra. The angle between the two anterior edges ($>110^\circ$) is larger than in
360 *Nanhsiungchelys wuchingensis* ($\sim 100^\circ$) (Tong & Li, 2019). The only identifiable scutes are the
361 gular and the humeral. In many nanhsiungchelyids, like *Basilemys praeclara*, *B. morrinensis*,
362 *Jiangxichelys ganzhouensis*, *J. neimongolensis*, *Hanbogdemys orientalis*, *Zangerlia*
363 *dzamynchondi* and *Kharakhutulia kalandadzei* (Brinkman & Nicholls, 1993; Brinkman & Peng,
364 1996; Sukhanov, 2000; Sukhanov et al., 2008; Danilov et al., 2013; Tong et al., 2016; Mallon &
365 Brinkman, 2018), extragular scutes usually occur beside the gular scutes, but this does not occur
366 in *Nanhsiungchelys wuchingensis* (Tong & Li, 2019) and *N. yangi*. Moreover, the location and
367 shape of the sulci of *Nanhsiungchelys yangi* are similar to those seen in *N. wuchingensis* (Tong
368 & Li, 2019). In *Nanhsiungchelys yangi*, the sulcus between the gular and humeral scutes can be
369 identified, and it is slightly curved and extend onto the entoplastron, which is similar to the
370 configuration seen in *Jiangxichelys neimongolensis* and *Nanhsiungchelys wuchingensis*
371 (Brinkman & Peng, 1996; Brinkman et al., 2015; Tong & Li, 2019). However, in the other
372 nanhsiungchelyids (e.g., *Kharakhutulia kalandadzei*, *Zangerlia dzamynchondi*, *Hanbogdemys*
373 *orientalis*, *Yuchelys nanyangensis* and *Jiangxichelys ganzhouensis*), this sulcus is tangential to
374 (or separated from) the entoplastron (Sukhanov, 2000; Sukhanov et al., 2008; Tong et al., 2012;
375 Danilov et al., 2013; Tong et al., 2016).

376

377 Discussion

378 Taxonomy

379 Through comparison with a complete specimen (IVPP V3106) of *Nanhsiungchelys*
380 *wuchingensis*, the large skull (length = 13 cm) of CUGW VH108 is inferred to correspond to an
381 entire carapace length of ~ 55.5 cm (see Fig. 5A for a definition of ‘entire carapace length’, which
382 comes from Hirayama et al. (2001)). This large body size, coupled with the network of
383 sculptures on the surface of the skull and shell, clearly demonstrates that CUGW VH108 belongs
384 to Nanhsiungchelyidae (Li & Tong, 2017). Moreover, CUGW VH108 has a laterally thickened
385 epiplastron (Fig. 2), with the anterior edge of the epiplastron extending anterior of the deepest
386 part of nuchal emargination (Fig. 4), additional features that are diagnostic of
387 Nanhsiungchelyidae (Li & Tong, 2017).

388 Within Nanhsiungchelyidae, CUGW VH108 differs from *Basilemys*, *Hanbogdemys*,
389 *Kharakhutulia*, *Yuchelys*, and *Zangerlia* because all of these taxa have weak nuchal emargination
390 and/or lack distinct anterolateral processes (Mlynarski, 1972; Sukhanov, 2000; Sukhanov et al.,
391 2008; Tong et al., 2012; Danilov et al., 2013; Mallon & Brinkman, 2018). Moreover, CUGW
392 VH108 differs from *Jiangxichelys ganzhouensis* and *J. neimongolensis* in which the cheek
393 emargination and temporal emargination are deep (Brinkman & Peng, 1996; Tong et al., 2016).
394 Although the carapace of both *Anomalochelys* and CUGW VH108 have deep nuchal
395 emargination and a pair of anterolateral processes, the former’s anterolateral processes are

396 slender crescent-shaped and have a bifurcated anterior end (*Hirayama et al., 2001*), which are
397 clear differences from the wide processes of CUGW VH108.

398 CUGW VH108 is assigned to the genus *Nanhsiungchelys* based on the deep nuchal
399 emargination, pair of anterolateral processes, and weakly developed cheek emargination and
400 temporal emargination (*Li & Tong, 2017*). However, CUGW VH108 differs from
401 *Nanhsiungchelys wuchingensis* in which the snout is trumpet shaped (*Tong & Li, 2019*).
402 Moreover, *Nanhsiungchelys wuchingensis* and CUGW VH108 show some differences in their
403 skeletal features (Table 2). In CUGW VH108 these include: the premaxilla is very small and
404 higher than it is wide (Fig. 3C–F); the top of the maxilla is straight (in lateral views) (Fig. 3C–F);
405 the maxilla does not occupy the space of the prefrontal (in dorsal views) (Fig. 3A, B); a small
406 portion of the maxilla extends posterior and ventral of the orbit (Fig. 3C–F); the parallelogram-
407 shaped jugal is greater in height than width (Fig. 3C–F); the prefrontal is convex dorsally behind
408 the apertura narium externa; the parietals are bigger than the frontals (Fig. 3A, B); the middle
409 and posterior parts of the mandible are more robust than the most anterior part in ventral view;
410 and the angle between the two anterior edges of the entoplastron is wide ($\sim 110^\circ$). It is possible
411 that the snout of the only known specimen of *Nanhsiungchelys wuchingensis* (IVPP V3106) was
412 deformed during the burial process, because its trumpet-shaped morphology has not been
413 reported in any other turtles. However, the post-cranial skeleton does not show much evidence of
414 post-mortem deformation, and both *Yeh (1966)* and *Tong & Li (2019)* regarded the unique snout
415 as an original, diagnostic characteristic. CUGW VH108 also differs from *Nanhsiungchelys* sp.
416 (SNHM 1558) in which the anterolateral processes are slender horn-shaped (*Hirayama et al.,*
417 *2009*). The anterior processes of the ‘Hefei specimen’ are believed to be long and similar to
418 those of *Anomalochelys angulata* (*Hu et al., 2016*), whereas these are relatively short in CUGW
419 VH108. Thus, CUGW VH108 differs from all other known species of Nanhsiungchelyidae, and
420 herein we erect the new species *Nanhsiungchelys yangi*. Lastly, on the basis of *Tong & Li (2019)*
421 and our new specimen, we emended the diagnosis of *Nanhsiungchelys*. Characteristics shared by
422 both *Nanhsiungchelys wuchingensis* and *N. yangi* are retained, and we exclude the characters
423 that do not match *N. yangi*, such as a long and trumpet-shaped snout, large frontal, and relatively
424 small parietal. This revised diagnosis is listed above.

425 The differences between *Nanhsiungchelys yangi* and *N. wuchingensis* are not likely to
426 represent ontogenetic variation. Despite only corresponding to half the length of
427 *Nanhsiungchelys wuchingensis* (IVPP V3106), the entire carapace length (~ 55.5 cm) of *N. yangi*
428 (CUGW VH108) is still in the middle of the size range reported among Nanhsiungchelyidae. For
429 instance, the entire carapace length of the Chinese nanhsiungchelyid *Jiangxichelys ganzhouensis*
430 is ~ 46 – 74 cm (*Tong et al., 2016*), and the estimated entire carapace length of adult
431 nanhsiungchelyid *Kharakhutulia kalandadzei* is only ~ 23 – 25 cm (*Sukhanov et al., 2008*). In
432 addition, juveniles usually have a larger skull relative to their carapace, whereas mature
433 individuals may have a relatively smaller skull (*Brinkman et al., 2013*). The ratios of maximum
434 head width (HW) to straightline carapace width (SCW) are $\sim 30\%$ in both *Nanhsiungchelys yangi*
435 (CUGW VH108) and *N. wuchingensis* (IVPP V3106) (*Tong & Li, 2019*).

436 Sexual dimorphism is another possible explanation of the observed differences between
437 *Nanhsiungchelys yangi* and *N. wuchingensis*, but this is very difficult to assess. *Cadena et al.*
438 (2020) suggested that horns (similar to the anterolateral processes in *Nanhsiungchelys*) could be
439 used to identify sex in the turtle *Stupendemys geographicus*. However, all known specimens of
440 *Nanhsiungchelys* exhibits distinct anterolateral processes. Some extant male tortoises (e.g.,
441 *Centrochelys sulcata*) have a more robust epiplastron than females (*Zhou & Zhou, 2020*), but
442 such a difference has not been reported in *Nanhsiungchelys*. Other lines of evidence (e.g.,
443 concavity of the plastron and shape of the xiphiplastral region) commonly used to determine the
444 sex of extant turtles (*Pritchard, 2007*) are also unavailable due to the poor preservation of the
445 above specimens. Based on above discussion, the most reasonable conclusion is that CUGW
446 VH108 represents a distinct species, rather than the product of intraspecific variation.

447

448 **Phylogenetic position and paleobiogeography**

449 The phylogenetic analysis retrieved seven most parsimonious trees with a length of 77 steps, a
450 consistency index (CI) of 0.675, and a retention index (RI) of 0.679. The strict consensus tree
451 (Fig. 6) recovers *Nanhsiungchelys yangi* and *N. wuchingensis* as sister taxa, with one
452 unambiguous synapomorphy identified: the absence of the extragulars. These two species and
453 *Anomalochelys angulata* form a monophyletic group, which is consistent with the results of *Tong*
454 & *Li (2019)*. Synapomorphies of this group include wide neurals, first vertebral scute with lateral
455 edges converging anteriorly, cervical scute as wide as long, and the length to width ratio of the
456 carapace is larger than 1.6. In particular, our new character (character 50, the length to width
457 ratio of the carapace) supports this relationship, suggesting it could prove informative in other
458 studies of turtle phylogeny. However, the standard bootstrap and Bremer supports values are low
459 among these groups, and their relationships therefore need further consideration. Interestingly,
460 our new results identify *Yuchelys nanyangensis* and *Zangerlia testudinimorpha* as sister taxa, and
461 this relationship was supported by one unambiguous synapomorphy (their fifth vertebral almost
462 fully covers the suprapygal). However, this relationship needs to be tested in future work because
463 the only known specimen of *Yuchelys nanyangensis* (HGM NR09-11-14) is poorly preserved
464 (*Tong et al., 2012*) and only 15 characters could be used in our phylogenetic analysis.

465 Although *Anomalochelys* and *Nanhsiungchelys* were in similar stages (Fig. 6), they appear to
466 have lived in different regions (southern China and Japan, respectively). In fact, Cretaceous turtle
467 communities in Japan and the rest of Asia (especially China and Mongolia) are closely
468 comparable, with both areas containing representatives of Adocusia, Lindholmemydidae,
469 Sinochelyidae, and Sinemydidae (*Hirayama et al., 2000*). Similar extinct organisms in these
470 regions also include the plant *Neozamites* (*Sun et al., 1993; Duan, 2005*), the bivalve
471 *Trigonioides* (*Ma, 1994; Komatsu et al., 2007*), and the dinosaur Hadrosaurinae (*Kobayashi et*
472 *al., 2019; Zhang et al., 2020*). *Sun & Yang (2010)* inferred that the Japan Sea did not exist during
473 the Jurassic and Cretaceous, with the Japan archipelago still closely linked to the eastern
474 continental margin of East Asia. This view is also supported by geological and geophysical
475 evidence (*Kaneoka et al., 1990; Liu et al., 2017*). In addition to *Anomalochelys angulata* from

476 Hokkaido (Hirayama *et al.*, 2001), many fragments of Nanhsiungchelyidae (as *Basilemys* sp.)
477 have also been found on Honshu and Kyushu islands, Japan (Hirayama, 1998; Hirayama, 2002;
478 Danilov & Syromyatnikova, 2008). In China, the easternmost specimen of a nanhsiungchelyid
479 turtle (a fragment of the shell) was recovered from the Upper Cretaceous of Laiyang, Shandong
480 (Li & Tong, 2017), which is near the west coast of the Pacific Ocean and close to Japan
481 geographically. This geographical proximity likely allowed nanhsiungchelyids to disperse
482 between China and Japan during the Late Cretaceous.

483

484 **Function of the anterolateral processes of the carapace**

485 The anterolateral processes of *Nanhsiungchelys* (and *Anomalochelys*) probably performed a
486 variety of functions, but the principal function was most likely self-protection. In the earliest
487 research on *Nanhsiungchelys wuchingensis*, Yeh (1966) did not discuss the function of the
488 anterolateral processes, but speculated that the neck was flexible, and the skull could be
489 withdrawn into the shell to avoid danger. This hypothesis was supported by a complete specimen
490 (93NMBY-2) of nanhsiungchelyid *Jiangxichelys neimongolensis* whose head was withdrawn
491 into the shell (Brinkman *et al.*, 2015). In contrast, Hirayama *et al.* (2001) suggested that the large
492 skull could not be fully withdrawn within the shell (parallel to the extant big-headed turtle
493 *Platysternon megacephalum*) and that the anterolateral processes of *Nanhsiungchelys*
494 *wuchingensis* and *Anomalochelys angulata* were used for protecting the skull. Hirayama *et al.*
495 (2001) also noted that *Nanhsiungchelys* has undeveloped temporal emargination, whereas
496 *Jiangxichelys* has distinct temporal emargination, and the former condition could inhibit the
497 ability to retract the skull inside the shell (Hirayama *et al.*, 2009; Werneburg, 2015; Hermanson
498 *et al.*, 2022). Together, this suggests that despite the possession of a flexible neck that could have
499 made it possible to retract the head, the large size of the skull and the reduced temporal
500 emargination were considerable obstacles to doing so. Today, turtles that cannot retract the head
501 are restricted to a few aquatic groups (e.g., Platysternidae) (Zhou & Li, 2013), whereas most
502 turtles (including all tortoises) have this capability (Zhou & Zhou, 2020). An additional strong
503 piece of evidence that *Nanhsiungchelys* could not retract the head is that the skulls of all known
504 specimens (IVPP V3106, SNHM 1558, and CUGW VH108) are preserved outside of the shell,
505 and the anterolateral processes would thus provide lateral protection for the head (Yeh, 1966;
506 Hirayama *et al.*, 2009; Tong & Li, 2019). Nevertheless, it seems evident that this protective
507 strategy of *Nanhsiungchelys* was inefficient, because the dorsal side of the head would be left
508 vulnerable to attack, and this may explain why extant terrestrial turtles usually abandon this
509 mode of protection.

510 The anterolateral processes might also have been used during fighting for mates, as
511 hypothesized for the extinct side-necked turtle *Stupendemys geographicus* (Cadena *et al.*, 2020).
512 Nanhsiungchelyids and extant tortoises share many comparable skeletal characteristics
513 (Hutchison & Archibald, 1986) and inferred reproductive behaviors (Ke *et al.*, 2021), and thus
514 *Nanhsiungchelys* might have been characterized by similar combat behavior. A parallel
515 hypothesis was proposed by Hirayama & Sonoda (2012) that the combinations of cranial and

516 nuchal morphology in *Nanhsiungchelys* and *Anomalochelys* could facilitate sexual displays,
517 similar to some extant testudinids. However, all known specimens of *Nanhsiungchelys* and
518 *Anomalochelys* possess distinct anterolateral processes and deep nuchal emargination, suggesting
519 these structures might also have been present in females (although this is uncertain because it is
520 not possible to determine their sex). If so, the anterolateral processes would not be the result of
521 sexual dimorphism and associated combat or display. Another piece of evidence arguing against
522 the fighting view is that there are no scars on the anterolateral processes of CUGW VH108, as
523 might be expected if they were used in fighting.

524 The anterolateral processes of *Nanhsiungchelys* might also have had a secondary function in
525 reducing drag as the animal was moving through water. Today, some tortoises living in dry areas
526 (e.g., *Aldabrachelys gigantea* and *Centrochelys sulcata*) will immerse themselves in mud or
527 water for a long time to avoid the hot weather (Zhou & Zhou, 2020), and *Aldabrachelys gigantea*
528 could even swim (or float) in the ocean (Gerlach et al., 2006; Hansen et al., 2016). Nanxiong
529 Basin was extremely hot (~27–34 °C) during the Late Cretaceous (Yang et al., 1993), and the
530 appearance of diverse fossils of Gastropoda, Bivalvia, Charophyceae, and Ostracoda (Zhang et
531 al., 2013) suggests the existence of lakes or rivers. Thus, *Nanhsiungchelys* may have had a
532 parallel lifestyle to these tortoises, and the reduction of drag could have been important under
533 these circumstances. Nessov (1984) also mentioned that nanhsiungchelyids would anchor
534 themselves on the bottom of streams to offset drift, which could be an adaptation to strong
535 currents. The anterolateral processes of *Nanhsiungchelys* could have played a role in reducing
536 resistance to fluid motion, and the efficiency of this would have been close to the level of extant
537 freshwater turtles (see Supplemental Information 3 for detailed information on hydrodynamic
538 analyses). The reason for this is that these processes made the anterior part of the shell more
539 streamlined (Fig. 7A, B), analogous to the streamlined fairing on the anterior of airplanes and
540 rockets. However, we acknowledge this remains a hypothesis at this time, because there is no
541 conclusive evidence of swimming in *Nanhsiungchelys*.

542 Many of the specialized morphological features of nanhsiungchelyids (e.g., huge skull, distinct
543 anterolateral processes, and unusually thick eggshells) are most likely adaptations to their
544 environment. *Nanhsiungchelys* was a successful genus because it belongs to the only group of
545 turtles that has been reported from the Dafeng Formation, suggesting these unusual turtles were
546 well adapted to their environment. However, their specialist survival strategies might have been
547 very inefficient, because the anterolateral processes could not protect the dorsal side of the head,
548 and the thick eggshell (Ke et al., 2021) might have hindered the breathing and hatching of young.
549 All of these features are not present in extant turtles, suggesting this was not a dominant
550 direction in turtle evolution. Consistent with this, nanhsiungchelyids became extinct at the end of
551 the Cretaceous, but many contemporary turtles (e.g., Adocidae, Lindholmemydidae, and
552 Trionychidae) survived into the Cenozoic (Lichtig & Lucas, 2016).

553

554 Conclusions

555 A turtle skeleton (CUGW VH108) with a well-preserved skull and lower jaw, together with
556 the anterior parts of the shell, was found in Nanxiong Basin, China. This is assigned to the genus
557 *Nanhsiungchelys* based on the large estimated body size (~55.5 cm), the presence of a network
558 of sculptures on the surface of the skull and shell, shallow cheek emargination and temporal
559 emargination, deep nuchal emargination, and a pair of anterolateral processes on the carapace.
560 Based on the character combination of a triangular-shaped snout (in dorsal view) and wide
561 anterolateral processes, we erect a new species *Nanhsiungchelys yangi*. A phylogenetic analysis
562 of nanhsiungchelyids places *Nanhsiungchelys yangi* and *N. wuchingensis* as sister taxa. We agree
563 with previous suggestions that the anterolateral processes on the carapace could have protected
564 the head, but also infer a potential secondary function for reducing drag force during movement
565 through water. These unique characteristics might have helped nanhsiungchelyids survive in a
566 harsh environment, but did not save them from extinction during the K-Pg event.
567

568 Acknowledgements

569 We thank Xing Xu (IVPP) for his useful suggestions, thank Kaifeng Wu (YSNHM) for
570 preparing turtle skeleton, and thank Mingbo Wang (UPC), Zichuan Qin (UB), Wen Deng
571 (CUGW) and Haoran Sun (LJU) for assistance with CFD.
572

573 References

- 574 **Bell MA, Lloyd GT. 2014.** strap: an R package for plotting phylogenies against stratigraphy and
575 assessing their stratigraphic congruence. *Palaeontology* **58**:379-389. DOI:10.1111/pala.12142
- 576 **Bremer K. 1994.** Branch support and tree stability. *Cladistics* **10**:295-304. DOI:10.1111/j.1096-
577 0031.1994.tb00179.x
- 578 **Brinkman D, Nicholls EL. 1993.** New specimen of *Basilemys praeclara* Hay and its bearing on
579 the relationships of the Nanhsiungchelyidae (Reptilia: Testudines). *Journal of Paleontology*
580 **67**:1027-1031. DOI:10.1017/s002233600002535x
- 581 **Brinkman D, Peng J-H. 1996.** A new species of *Zangerlia* (Testudines: Nanhsiungchelyidae)
582 from the Upper Cretaceous redbeds at Bayan Mandahu, Inner Mongolia, and the relationships
583 of the genus. *Canadian Journal of Earth Sciences* **33**:526-540. DOI:10.1139/e96-041
- 584 **Brinkman DB, Tong H-Y, Li H, Sun Y, Zhang J-S, Godefroit P, Zhang Z-M. 2015.** New
585 exceptionally well-preserved specimens of “*Zangerlia*” *neimongolensis* from Bayan Mandahu,
586 Inner Mongolia, and their taxonomic significance. *Comptes Rendus Palevol* **14**:577-587.
587 DOI:10.1016/j.crpv.2014.12.005
- 588 **Brinkman DB, Yuan C-X, Ji Q, Li D-Q, You H-L. 2013.** A new turtle from the Xiagou
589 Formation (Early Cretaceous) of Changma Basin, Gansu Province, P. R. China.
590 *Palaeobiodiversity and Palaeoenvironments* **93**:367-382. DOI:10.1007/s12549-013-0113-0
- 591 **Bureau of Geology and Mineral Exploration and Development of Jiangxi Province. 2017.**
592 *Regional geology of China, Jiangxi Province*. Beijing: Geological Publishing House. (in
593 Chinese with English abstract)
- 594 **Cadena E-A, Scheyer TM, Carrillo-Briceño JD, Sánchez R, Aguilera-Socorro OA, Vanegas**

- 595 **A, Pardo M, Hansen DM, Sánchez-Villagra MR. 2020.** The anatomy, paleobiology, and
596 evolutionary relationships of the largest extinct side-necked turtle. *Science Advances*
597 **6**:eaay4593. DOI:10.1126/sciadv.aay4593
- 598 **Danilov IG, Sukhanov VB, Syromyatnikova EV. 2013.** Redescription of *Zangerlia*
599 *dzamynchondi* (Testudines: Nanhsiungchelyidae) from the Late Cretaceous of Mongolia, with
600 a reassessment of the phylogenetic position and relationships of *Zangerlia*. *Morphology and*
601 *Evolution of Turtles*, 407-417.
- 602 **Danilov IG, Syromyatnikova EV. 2008.** New materials on turtles of the family
603 Nanhsiungchelyidae from the Cretaceous of Uzbekistan and Mongolia, with a review of the
604 nanhsiungchelyid record in Asia. *Proceedings of the Zoological Institute RAS* **312**:3-25.
- 605 **Duan Y. 2005.** A new material of *Neozamites* from Yixian Formation of western Liaoning and
606 its paleophytogeographic significance. *Global Geology* **24**:112-116. (in Chinese with English
607 abstract)
- 608 **Gerlach J, Muir C, Richmond MD. 2006.** The first substantiated case of trans-oceanic tortoise
609 dispersal. *Journal of Natural History* **40**:2403-2408. DOI:10.1080/00222930601058290
- 610 **Goloboff PA, Catalano SA. 2016.** TNT version 1.5, including a full implementation of
611 phylogenetic morphometrics. *Cladistics* **32**:221-238. DOI: 10.1111/cla.12160
- 612 **Guangdong Geological Survey Institute. 2017.** *Regional geology of Guangdong, Xianggang,*
613 *and Aomen (second edition)*. (in Chinese)
- 614 **Hansen DM, Austin JJ, Baxter RH, Boer EJD, Falcón W, Norder SJ, Rijdsdijk KF, Thébaud**
615 **C, Bunbury NJ, Warren BH. 2016.** Origins of endemic island tortoises in the western Indian
616 Ocean: a critique of the human-translocation hypothesis. *Journal of Biogeography* **44**:1430–
617 1435. DOI:10.1111/jbi.12893
- 618 **Hermanson G, Benson RBJ, Farina BM, Ferreira GS, Langer MC, Evers SW. 2022.** Cranial
619 ecomorphology of turtles and neck retraction as a possible trigger of ecological diversification.
620 *Evolution*:1-21. DOI: 10.1111/evo.14629
- 621 **Hirayama R. 1998.** Fossil turtles from the Mifune Group (Late Cretaceous) of Kumamoto
622 Prefecture, Western Japan. Report of the research on the distribution of important fossils in
623 Kumamoto Prefecture: Dinosaurs from the Mifune Group, Kumamoto Prefecture, Japan: 85-
624 99. (in Japanese with English abstract)
- 625 **Hirayama R. 2002.** Preliminary report of the fossil turtles from the Kitadani Formation (Early
626 Cretaceous) of the Tetori Group of Katsuyama, Fukui Prefecture, Central Japan. *Memoir of the*
627 *Fukui Prefectural Dinosaur Museum* **1**:29-40. (in Japanese with English abstract)
- 628 **Hirayama R, Brinkman DB, Danilov IG. 2000.** Distribution and biogeography of non-marine
629 Cretaceous turtles. *Russian Journal of Herpetology* **7**:181–198.
- 630 **Hirayama R, Sakurai K, Chitoku T, Kawakami G, Kito N. 2001.** *Anomalocheilus angulata*,
631 an unusual land turtle of family Nanhsiungchelyidae (superfamily Trionychoidea; order
632 Testudines) from the Upper Cretaceous of Hokkaido, North Japan. *Russian Journal of*
633 *Herpetology* **8**:127-138.
- 634 **Hirayama R, Sonoda T. 2012.** Morphology and evolution of Nanhsiungchelyidae (Cryptodira:

- 635 Trionychia). [Abstract] *Symposium on Turtle Evolution*: 21.
- 636 **Hirayama R, Zhong Y, Di Y, Yonezawa T, Hasegawa M. 2009.** A new nanhsiungchelyid
637 turtle from Late Cretaceous of Guangdong, China. In: Brinkman D, ed. *Gaffney Turtle*
638 *Symposium*: Drumheller: Royal Tyrell Museum, 72-73.
- 639 **Hu Y, Huang J, Obratzsova EM, Syromyatnikova EV, Danilov IG. 2016.** A new
640 nanhsiungchelyid turtle from the Late Cretaceous of Jiangxi, China. [Abstract] *SVP 76th*
641 *Annual meeting*: 158.
- 642 **Hutchison JH, Archibald JD. 1986.** Diversity of turtles across the Cretaceous/Tertiary
643 boundary in northeastern Montana. *Palaeogeography, Palaeoclimatology, Palaeoecology*
644 **55**:1-22. DOI:10.1016/0031-0182(86)90133-1
- 645 **Jerzykiewicz T, Currie PJ, Eberth DA, Johnsto PA, Koster EH, Zheng J-J. 1993.** Djadokhta
646 Formation correlative strata in Chinese Inner Mongolia: an overview of the stratigraphy,
647 sedimentary geology, and paleontology and comparisons with the type locality in the pre-Altai
648 Gobi. *Canadian Journal of Earth Science* **30**:2180-2195. DOI:10.1139/e93-190
- 649 **Joyce WG, Anquetin J, Cadena E-A, Claude J, Danilov IG, Evers SW, Ferreira GS, Gentry**
650 **AD, Georgalis GL, Lyson TR, Pérez-García A, Rabi M, Sterli J, Vitek NS, Parham JF.**
651 **2021.** A nomenclature for fossil and living turtles using phylogenetically defined clade names.
652 *Swiss Journal of Palaeontology* **140**:1-45. DOI:10.1186/s13358-020-00211-x
- 653 **Joyce WG, Norell MA. 2005.** *Zangerlia ukhaachelys*, new species, a nanhsiungchelyid turtle
654 from the Late Cretaceous of Ukhaa Tolgod, Mongolia. *American Museum Novitates* **3481**:1-
655 20. DOI:10.1206/0003-0082(2005)481[0001:Zunsan]2.0.Co;2
- 656 **Kaneoka I, Notsu K, Takigami Y, Fujioka K, Sakai H. 1990.** Constraints on the evolution of
657 the Japan Sea based on ⁴⁰Ar-³⁹Ar ages and Sr isotopic ratios for volcanic rocks of the Yamato
658 Seamount chain in the Japan Sea. *Earth and Planetary Science Letters* **97**:211-225.
659 DOI:10.1016/0012-821x(90)90109-b
- 660 **Ke Y, Wu R, Zelenitsky DK, Brinkman D, Hu J, Zhang S, Jiang H, Han F. 2021.** A large
661 and unusually thick-shelled turtle egg with embryonic remains from the Upper Cretaceous of
662 China. *Proceedings of the Royal Society B-Biological Sciences* **288**:20211239.
663 DOI:10.1098/rspb.2021.1239
- 664 **Kobayashi Y, Nishimura T, Takasaki R, Chiba K, Fiorillo AR, Tanaka K, Chinzorig T,**
665 **Sato T, Sakurai K. 2019.** A new hadrosaurine (Dinosauria: Hadrosauridae) from the marine
666 deposits of the Late Cretaceous Hakobuchi Formation, Yezo Group, Japan. *Scientific reports*
667 **9**:1-14. DOI:10.1038/s41598-019-48607-1
- 668 **Komatsu T, Jinhua C, Ugai H, Hirose K. 2007.** Notes on non-marine bivalve *Trigonioides*
669 (*Trigonioides*?) from the mid-Cretaceous Goshoura Group, Kyushu, Japan. *Journal of Asian*
670 *Earth Sciences* **29**:795–802. DOI:10.1016/j.jseas.2006.06.001
- 671 **Li J, Tong H. 2017.** *Palaeovertebrata sinica, volume II, amphibians, reptilians, and avians,*
672 *fascicle 2 (serial no. 6), parareptilians, captorhines, and testudines.* Beijing: Science Press. (in
673 Chinese)
- 674 **Lichtig AJ, Lucas SG. 2016.** Cretaceous nonmarine turtle biostratigraphy and evolutionary

- 675 events. *Cretaceous Period: Biotic Diversity and Biogeography New Mexico Museum of*
676 *Natural History and Science Bulletin* **71**:185-194.
- 677 **Ling Q, Zhang X, Lin J. 2005.** New advance in the study of the Cretaceous and Paleogene
678 strata of the Nanxiong Basin. *Journal of Stratigraphy* **29**:596-601. (in Chinese with English
679 abstract)
- 680 **Liu M, Wei D, Shi Y. 2017.** Review on the opening and evolution models of the Japan sea.
681 *Progress in Geophysics* **32**:2341-2352. (in Chinese with English abstract)
- 682 **Ma Q. 1994.** Nonmarine Cretaceous bivalve assemblages in China. *Cretaceous Research*
683 **15**:271-284. DOI:10.1006/cres.1994.1017
- 684 **Mallon JC, Brinkman DB. 2018.** *Basilemys morrinensis*, a new species of nanhsiungchelyid
685 turtle from the Horseshoe Canyon Formation (Upper Cretaceous) of Alberta, Canada. *Journal*
686 *of Vertebrate Paleontology* **38**:e1431922. DOI:10.1080/02724634.2018.1431922
- 687 **Mlynarski M. 1972.** *Zangerlia testudinimorpha* n. gen., n. sp., a primitive land tortoise from the
688 Upper Cretaceous of Mongolia. *Palaeontologia Polonica* **27**:85-92.
- 689 **Nessov LA. 1984.** Data on Late Mesozoic turtles from the USSR. *Studia Geologica*
690 *Salmanticensia especial* **1**:215-233.
- 691 **Pritchard PCH. 2007.** Evolution and structure of the turtle shell. In: Wyneken J, Godfrey MH,
692 and Bels V, eds. *Biology of turtles*. Boca Raton, FL: CRC Press, 45-84.
- 693 **Sukhanov VB. 2000.** Mesozoic turtles of Middle and Central Asia. In: Benton MJ, Shishkin MA,
694 Unwin DM, and Kurochkin EN, eds. *The age of dinosaurs in Russia and Mongolia*.
695 Cambridge: Cambridge University Press, 309-367.
- 696 **Sukhanov VB, Danilov IG, and Syromyatnikova EV. 2008.** The description and phylogenetic
697 position of a new nanhsiungchelyid turtle from the Late Cretaceous of Mongolia. *Acta*
698 *Palaeontologica Polonica* **53**:601-614. DOI:10.4202/app.2008.0405
- 699 **Sun G, Nakazawa T, Ohana T, Kimura T. 1993.** Two *Neozamites* species (Bennettitales) from
700 the Lower Cretaceous of Northeast China and the inner zone of Japan. *Transactions and*
701 *proceedings of the Paleontological Society of Japan New series* **172**:264-276.
- 702 **Sun G, Yang T. 2010.** Paleontological evidence-based discussion on the origin of the Japan Sea.
703 *Marine Sciences* **34**:89-92. (in Chinese)
- 704 **Syromyatnikova EV, Danilov IG. 2009.** New material and a revision of turtles of the genus
705 *Adocus* (Adocidae) from the Late Cretaceous of middle Asia and Kazakhstan. *Proceedings of*
706 *the Zoological Institute RAS* **313**:74-94.
- 707 **Tong H, Li L. 2019.** A revision of the holotype of *Nanhsiungchelys wuchingensis*, Ye, 1966
708 (Testudines: Cryptodira: Trionychoidea: Nanhsiungchelyidae). *Cretaceous Research* **95**:151-
709 163. DOI:10.1016/j.cretres.2018.11.003
- 710 **Tong H, Li L, Jie C, Yi L. 2016.** New material of *Jiangxichelys ganzhouensis* Tong & Mo,
711 2010 (Testudines: Cryptodira: Nanhsiungchelyidae) and its phylogenetic and
712 palaeogeographical implications. *Geological Magazine* **154**:456-464.
713 DOI:10.1017/s0016756816000108
- 714 **Tong H, Mo J. 2010.** *Jiangxichelys*, a new nanhsiungchelyid turtle from the Late Cretaceous of

- 715 Ganzhou, Jiangxi Province, China. *Geological Magazine* **147**:981-986.
716 DOI:10.1017/s0016756810000671
- 717 **Tong H, Xu L, Buffetaut E, Zhang X, Jia S. 2012.** A new nanhsiungchelyid turtle from the
718 Late Cretaceous of Neixiang, Henan Province, China. *Annales de Paléontologie* **98**:303-314.
719 DOI:10.1016/j.annpal.2012.08.001
- 720 **Wang W, Liu X, Ma M, Mao X, Ji J. 2016.** Sedimentary environment of Cretaceous red beds
721 in Nanxiong Basin, Guangdong Province. *Journal of Subtropical Resources and Environment*
722 **11**:29-37. (in Chinese with English abstract)
- 723 **Wang Y, Li Q, Bai B, Jin X, Mao F, Meng J. 2019.** Paleogene integrative stratigraphy and
724 timescale of China. *Science China Earth Sciences* **49**:289–314. (in Chinese)
- 725 **Werneburg I. 2015.** Neck motion in turtles and its relation to the shape of the temporal skull
726 region. *Comptes Rendus Palevol* **14**:527-548. DOI:10.1016/j.crpv.2015.01.007
- 727 **Xi D, Sun L, Qin Z, Li G, Li G, Wan X. 2021.** Lithostratigraphic subdivision and correlation of
728 the Cretaceous in China. *Journal of Stratigraphy* **45**:375-401. (in Chinese with English
729 abstract)
- 730 **Xu X, Pittman M, Sullivan C, Choiniere JN, Tan Q-W, Clark JM, Norell MA, Wang S.**
731 **2015.** The taxonomic status of the Late Cretaceous dromaeosaurid *Linheraptor exquisitus* and
732 its implications for dromaeosaurid systematics. *Vertebrata Palasiatica* **53**:29-62.
- 733 **Yang W, Chen N, Ni S, Nan J, Wu M, Jiang J, Ye J, Feng X, Ran Y. 1993.** Carbon and
734 oxygen isotopic composition and environmental significance of Cretaceous red-bed carbonate
735 rocks and dinosaur eggshells. *Chinese Science Bulletin* **38**:2161-2163. (in Chinese)
- 736 **Yeh H-K. 1966.** A new Cretaceous turtle of Nanhsiung, Northern Kwangtung. *Vertebrata*
737 *Palasiatica* **10**:191-200.
- 738 **Young C-C. 1965.** Fossil eggs from Nanhsiung, Kwangtung and Kanchou, Kiangsi. *Vertebrata*
739 *Palasiatica* **9**:141-159. (in Chinese with English abstract)
- 740 **Zanno LE. 2010.** A taxonomic and phylogenetic re-evaluation of Therizinosauria (Dinosauria:
741 Maniraptora). *Journal of Systematic Palaeontology* **8**:503–543.
742 DOI:10.1080/14772019.2010.488045
- 743 **Zhang X-q, Zhang X-m, Hou M-c, Li G, Li H-m. 2013.** Lithostratigraphic subdivision of red
744 beds in Nanxiong Basin, Guangdong, China. *Journal of Stratigraphy* **37**:441-451. (in Chinese
745 with English abstract)
- 746 **Zhang Y-G, Wang K-B, Chen S-Q, Liu D, Xing H. 2020.** Osteological re-assessment and
747 taxonomic revision of “*Tanius laiyangensis*” (Ornithischia: Hadrosauroidea) from the Upper
748 Cretaceous of Shandong, China. *The Anatomical Record* **303**:790-800.
749 DOI:10.1002/AR.24097
- 750 **Zhao Z, Wang Q, Zhang S. 2015.** *Palaeovertebrata Sinica, Volume II, Amphibians, Reptilians,*
751 *and Avians, Fascicle 7 (Serial no.11), Dinosaur Eggs.* Beijing: Science Press. (in Chinese)
- 752 **Zhao Z, Ye J, Li H, Zhao Z, Yan Z. 1991.** Extinction of dinosaurs at Cretaceous-Tertiary
753 boundary in Nanxiong Basin, Guangdong Province. *Vertebrata Palasiatica* **29**:1-12. (in
754 Chinese)

- 755 **Zhou T, Li P. 2013.** *Primary color illustrated handbook of classification of Chinese turtles.*
756 Beijing: China Agriculture Press. (in Chinese)
757 **Zhou T, Zhou F. 2020.** *Tortoises of the World.* Beijing: China Agriculture Press. (in Chinese)
758

Figure 1

Geological map of Nanxiong Basin and stratigraphic distribution of valid nanhsiungchelyid turtles in China.

(A) Geological map of Nanxiong Basin, and the red triangular indicates fossil site, after Wang et al. (2016), Wang et al. (2019) and Xi et al. (2021). (B) Stratigraphic distribution of valid nanhsiungchelyid turtles in China. Abbreviations: Cam, Campanian; Cen, Cenomanian; Con, Coniacian; Maa, Maastrichtian; San, Santonian; Tur, Turonian. Stratigraphic information based on work by the Bureau of Geology and Mineral Exploration and Development of Jiangxi Province (2017) , Guangdong Geological Survey Institute (2017) , Jerzykiewicz et al. (1993) , Xi et al. (2021) , and Xu et al. (2015) .

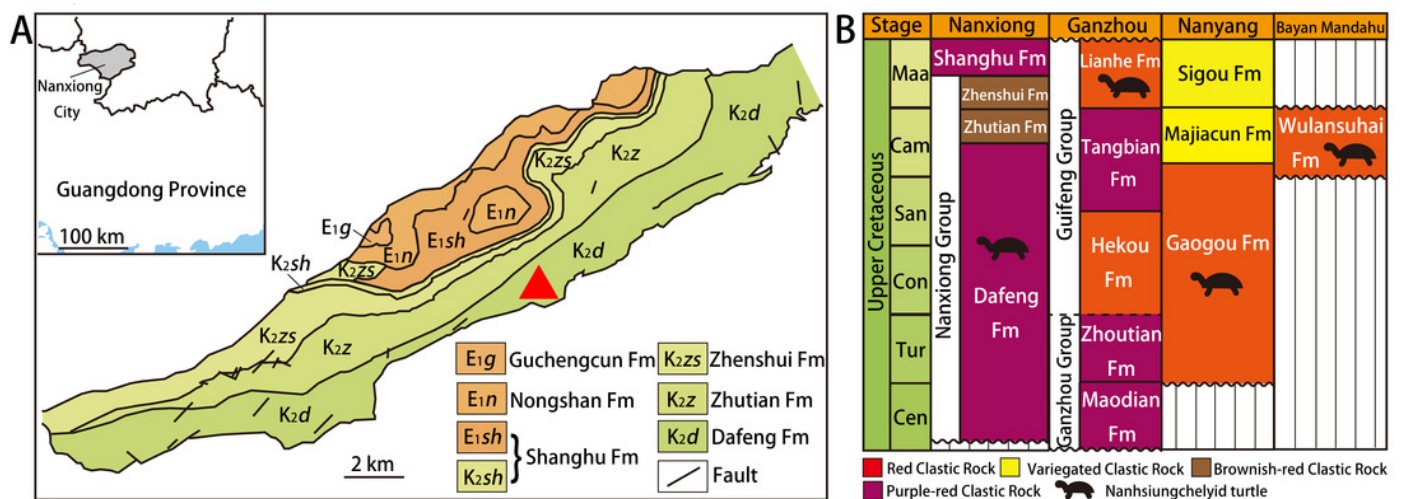


Figure 2

Photograph (A) and outline drawing (B) of *Nanhsiungchelys yangi* (CUGW VH108) in anterior view.

Gray and black parts indicate the surrounding rock and openings of the skull, respectively. Scale bar equals 5 cm. Abbreviations: ca, carapace; md, mandible; pl, plastron; sk, skull.

A



B

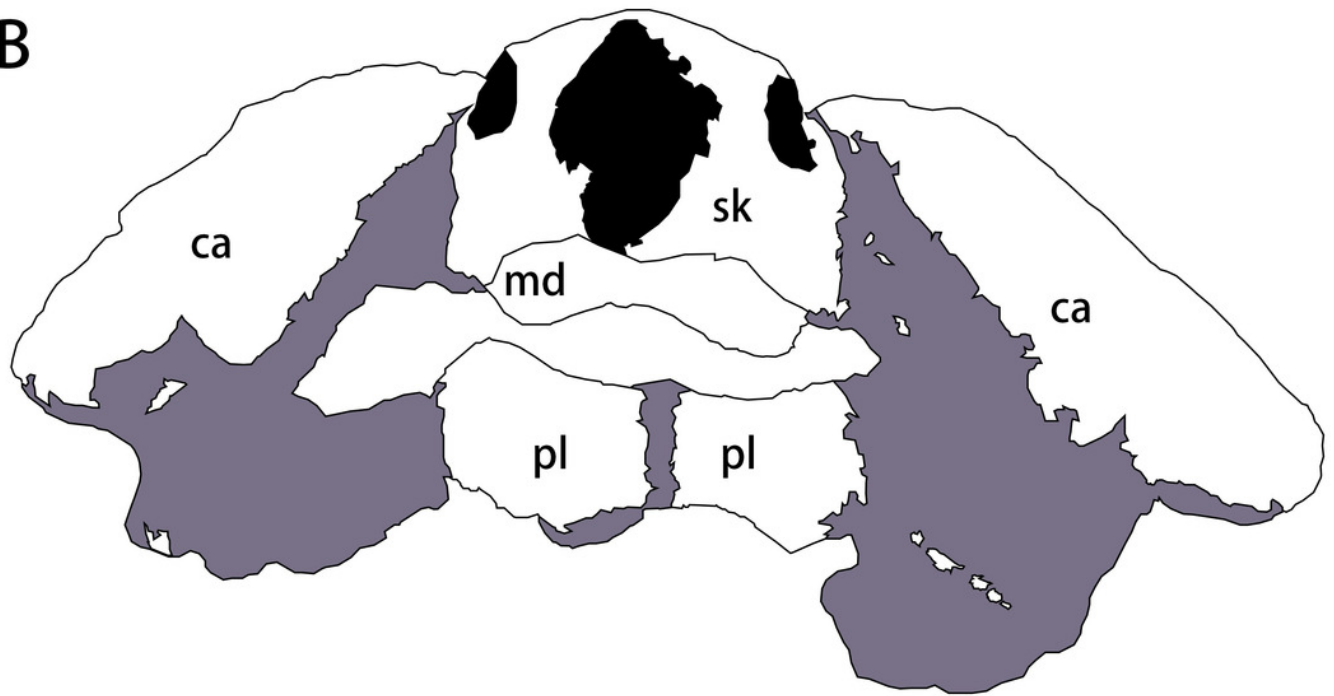


Figure 3

The skull and carapace of *Nanhsiungchelys yangi* (CUGW VH108).

(A, B) Photograph and outline drawing of the skull and carapace in dorsal view, with a magnified view showing a distinct protrusion at the tip of anterolateral process (perpendicular to the surface of the carapace). (C, D) Photograph and outline drawing of the skull in left lateral view. (E, F) Photograph and outline drawing of the skull in right lateral view. Gray and black parts indicate the surrounding rock and openings of the skull, respectively. Scale bars equal 5 cm. Abbreviations: ca, carapace; fr, frontal; ju, jugal; md, mandible; mx, maxilla; pa, parietal; pf, prefrontal; pm, premaxilla; po, postorbital; qj, quadratojugal.

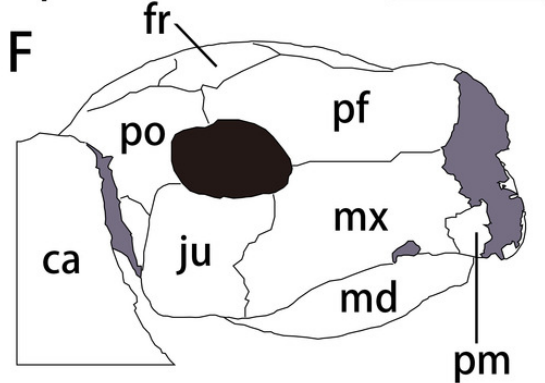
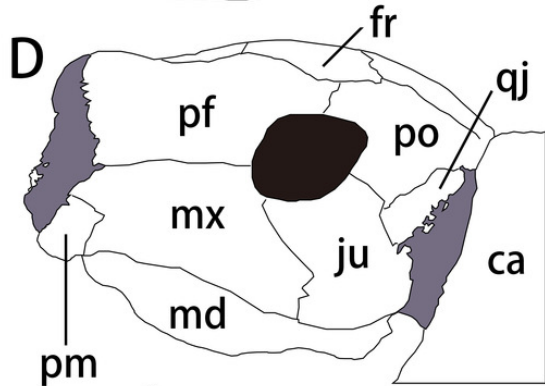
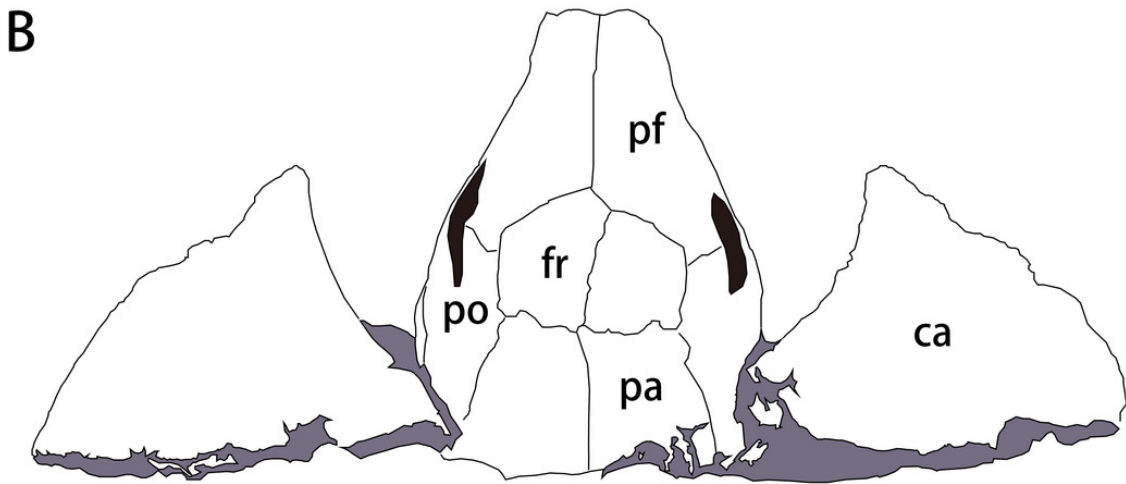
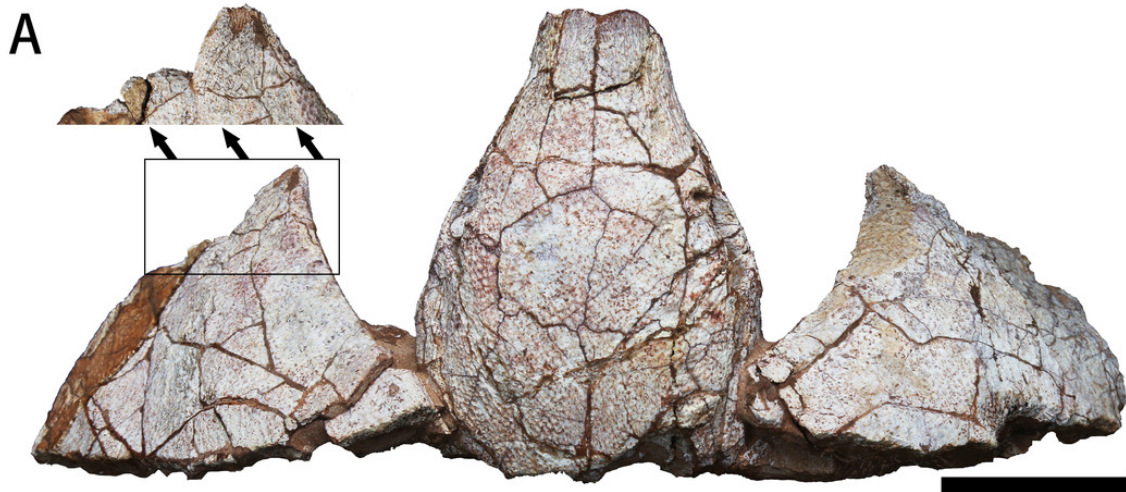


Figure 4

Photograph (A) and outline drawing (B) of *Nanhsiungchelys yangi* (CUGW VH108) in ventral view.

Bold lines represent the sulci between scutes and gray parts indicate the surrounding rock. Scale bar equals 5 cm. Abbreviations: ca, carapace; epi, epiplastron; ent, entoplastron; Gu, gular scute; Hum, humeral scute; md, mandible; sk, skull.

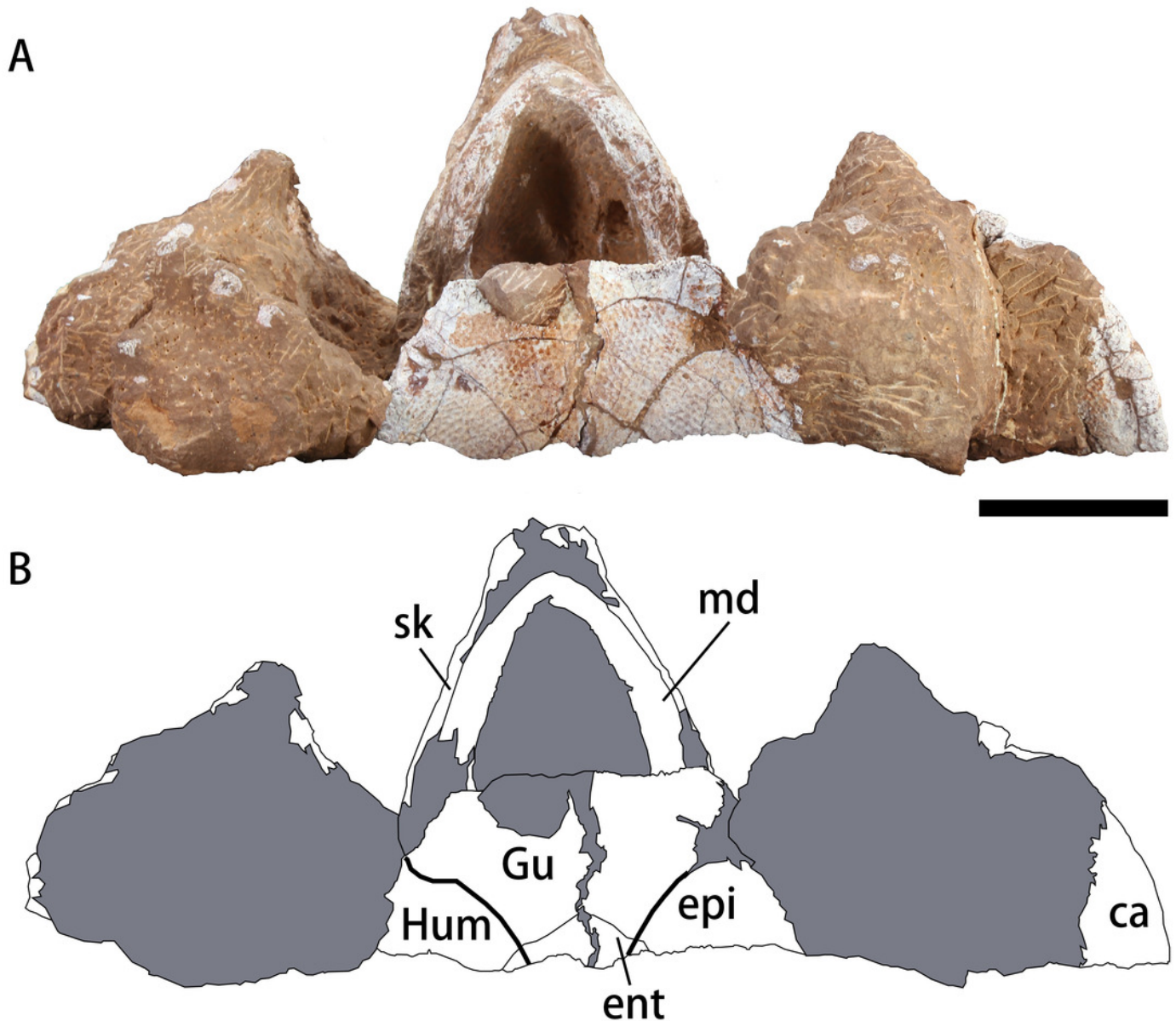


Figure 5

Outline drawings of three nanhsiungchelyids.

(A) Skull and carapace of *Nanhsiungchelys wuchingensis*, after Tong & Li (2019) and Hirayama et al. (2001). (B) Carapace of *Anomalochelys angulata*, after Hirayama et al. (2001). (C) Skull and partial carapace of *Nanhsiungchelys yangi* (CUGW VH108). (D) Skull of *Nanhsiungchelys wuchingensis* in left lateral view, after Tong & Li (2019); arrows indicate the concave prefrontal. (E) Skull of *Nanhsiungchelys yangi* (CUGW VH108) in left lateral view. Scale bars equal 10 cm. Bold black lines represent the sulci between scutes, thin gray lines indicate the sutures between bones, and dashed lines indicate a reconstruction of poorly preserved areas. Abbreviations: bones: art, articular; Bif, bifurcation; co, costal; den, dentary; fr, frontal; ju, jugal; mx, maxilla; md, mandible; n, neural; nu, nuchal; p, peripheral; pa, parietal; pf, prefrontal; pm, premaxilla; po, postorbital; Pro, protrusion; qj, quadratojugal; sq, squamosal; scutes: M, marginal scute; P, pleural scute; V, vertebral scute; measurement: ECL, entire carapace length; MHW, maximum head width; SCW, straightline carapace width.

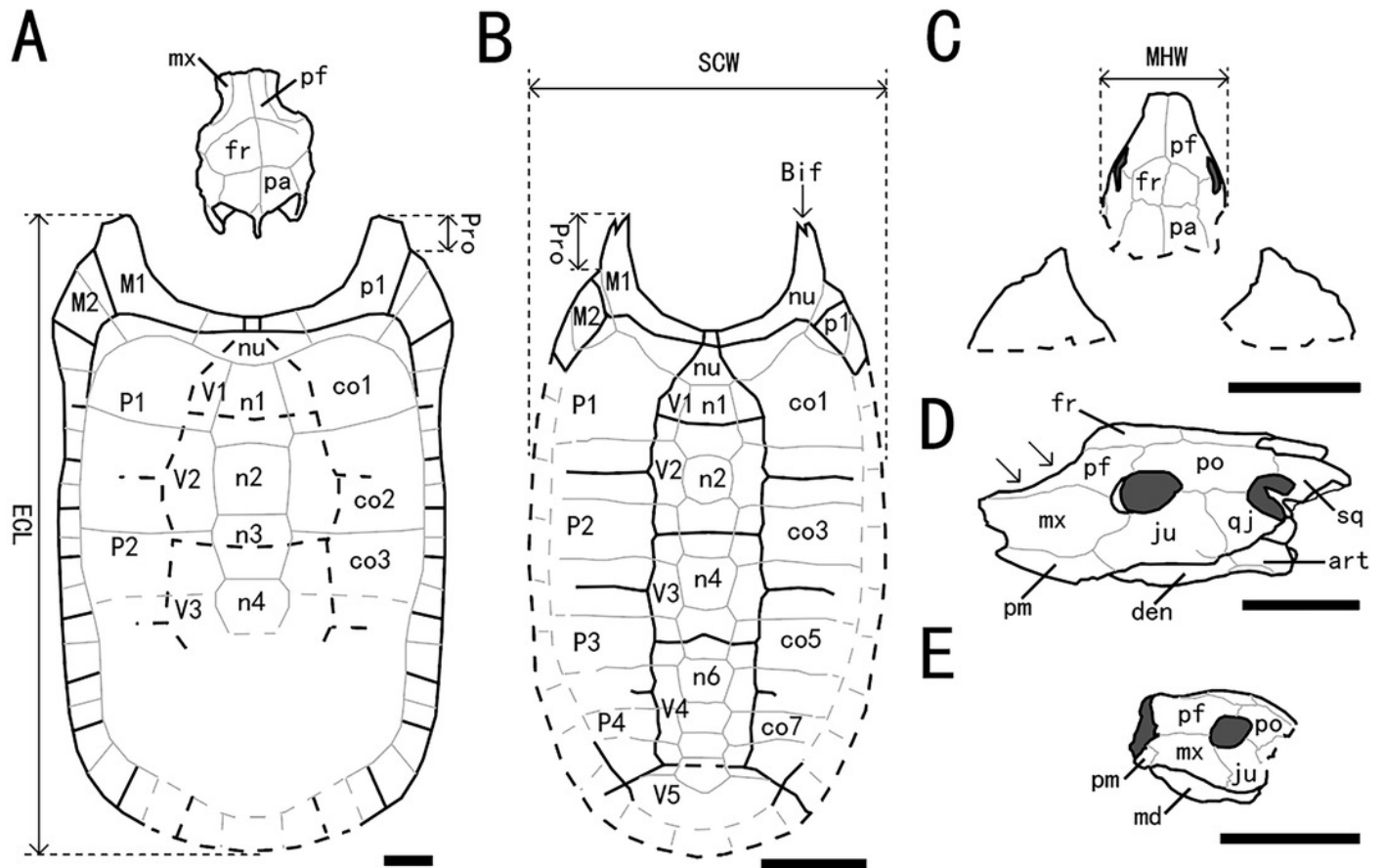


Figure 6

Time-scaled strict consensus tree of Nanhsiungchelyidae.

Numbers above nodes are bootstrap support values and numbers below nodes are Bremer support values. Please note that the bootstrap support values less than 50 and the Bremer support values equal to 1 are not shown here. Temporal distributions of species based on Danilov et al. (2013), Li & Tong (2017), Syromyatnikova & Danilov (2009), Tong et al. (2016), Mallon & Brinkman (2018), and Xi et al. (2021). Abbreviations: Hau, Hauterivian; Barr, Barremian; Apt, Aptian; Alb, Albian; Cen, Cenomanian; Tur, Turonian; Con, Coniacian; San, Santonian; Cam, Campanian; Maa, Maastrichtian; Dan, Danian; Sel, Selandian; Tha, Thanetian; Ypr, Ypresian; Lut, Lutetian; Bar, Bartonian; Pri, Priabonian; Rup, Rupelian; Cha, Chattian; Aqu, Aquitanian; Bur, Burdigalian.

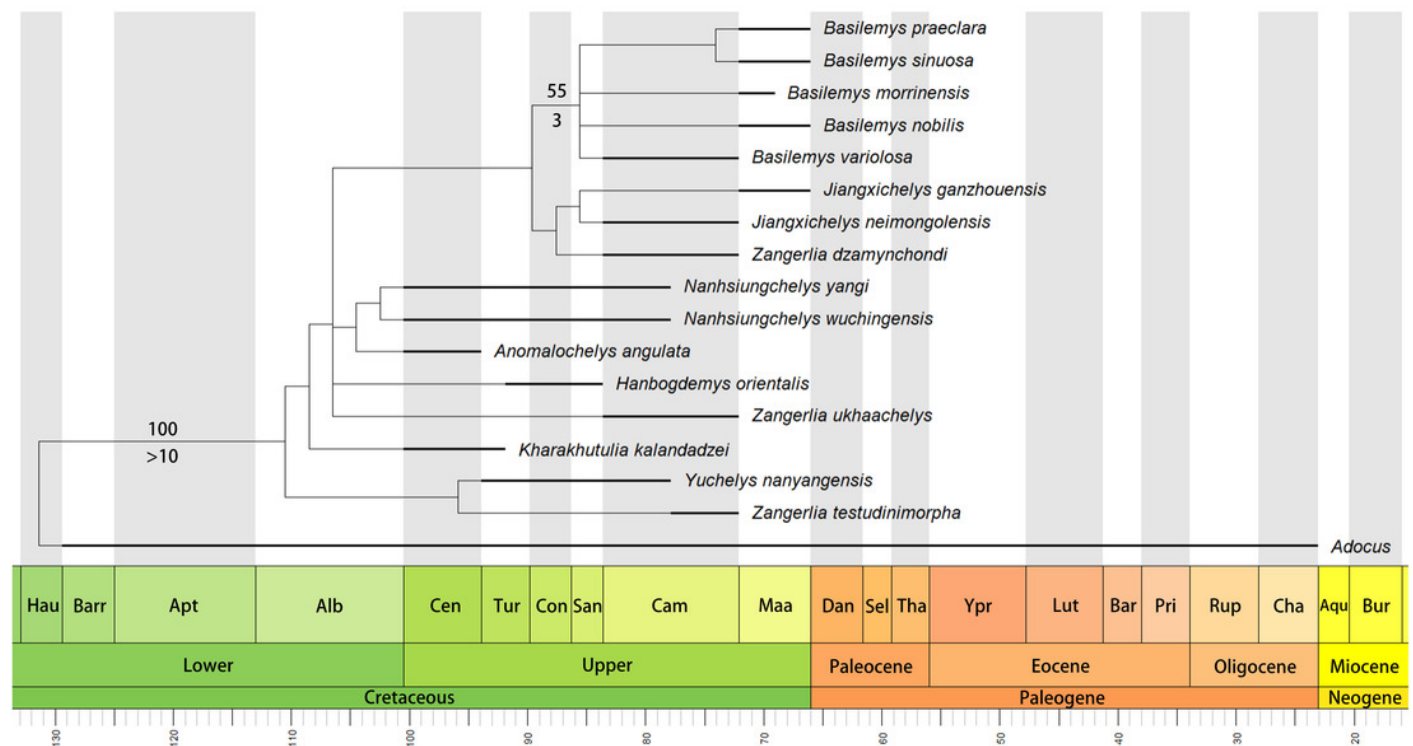


Figure 7

3-D plots of streamlines at flow velocities of 1.0 m s^{-1} .

(A) and (B) are the model of *Nanhsiungchelys yangi* (in left lateral and dorsal views, respectively); (C) and (D) are the model of hypothetical turtle I (in left lateral and dorsal views, respectively), whose anterior carapace and body are blunt; (E) and (F) are the model of hypothetical turtle II (in left lateral and dorsal views, respectively), whose anterior carapace is streamlined and similar to most freshwater turtles. The arrows indicate the anterolateral processes. The direction of ambient flow is from left to right.

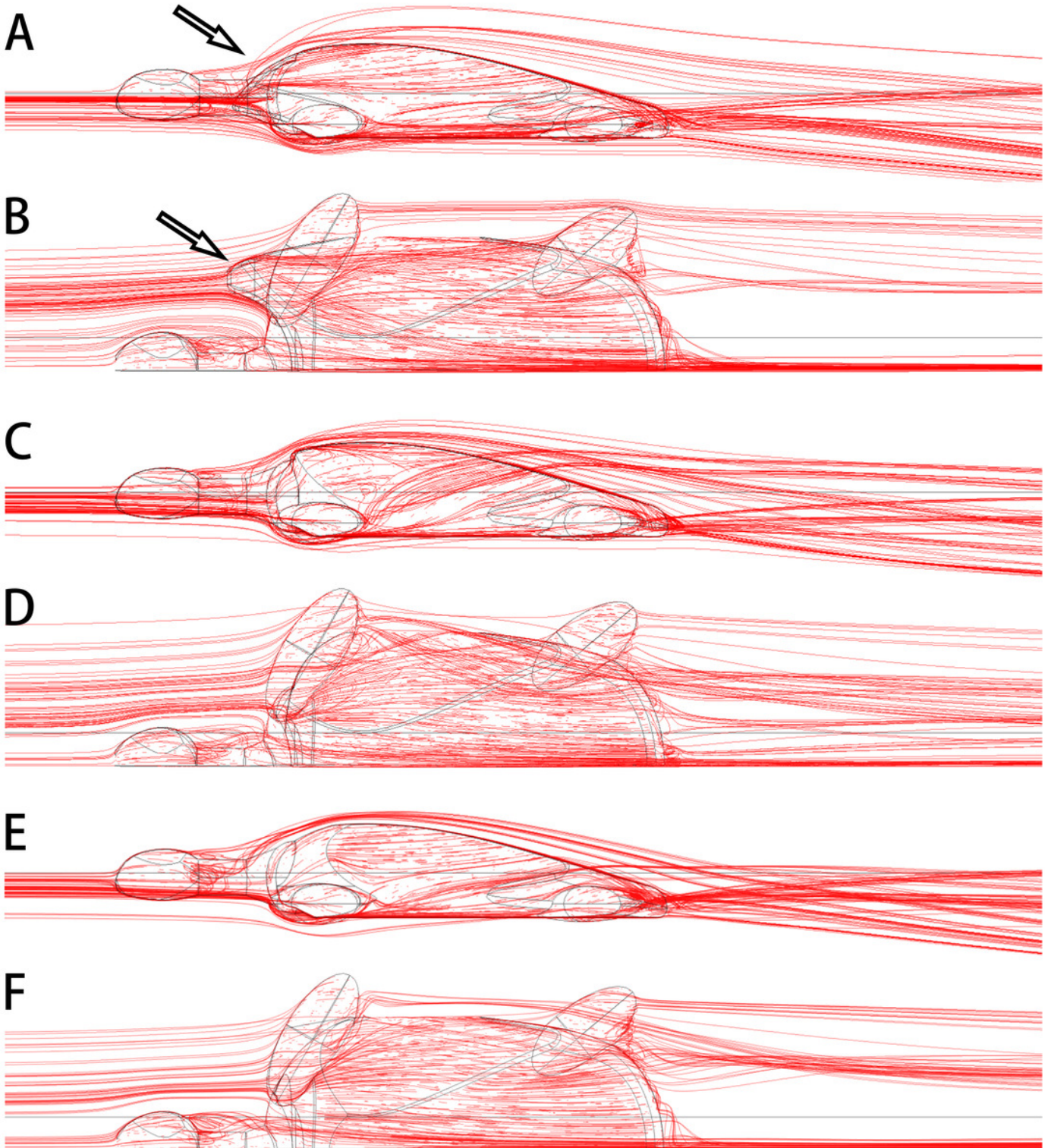


Table 1 (on next page)

Taxonomy and distribution of Nanhsiungchelyidae in China

Note: this table does not include small fragments which has less taxonomic significance.

- 1 Table 1:
2 Taxonomy and distribution of Nanhsiungchelyidae in China

Taxa	Specimen Number	Location	Age	Stratigraphic Unit	References
<i>Nanhsiungchelys wuchingensis</i>	IVPP V3106	Nanxiong, Guangdong	Late Cretaceous (Cenomanian–middle Campanian)	Dafeng Formation	<i>Yeh (1966)</i> <i>Tong & Li (2019)</i>
<i>Nanhsiungchelys</i> sp.	SNHM 1558	Nanxiong, Guangdong	Late Cretaceous (Cenomanian–middle Maastrichtian)	Nanxiong Group	<i>Hirayama et al. (2009)</i> <i>Li & Tong (2017)</i>
<i>Nanhsiungchelys yangi</i> sp. nov.	CUGW VH108	Nanxiong, Guangdong	Late Cretaceous (Cenomanian–middle Campanian)	Dafeng Formation	This paper
<i>Jiangxichelys neimongolensis</i>	IVPP RV96007, IVPP RV96008, IVPP 290690-6 RV 96009, IVPP 020790-4 RV 96010, IVPP 130790-1 RV 96011, IMM 4252, IMM 2802, IMM 96NMBY-I-14, IMM 93NMBY-2	Bayan Mandahu, Inner Mongolia	Late Cretaceous (Campanian)	Wulansuhai Formation	<i>Brinkman & Peng (1996)</i> <i>Brinkman et al. (2015)</i> <i>Li & Tong (2017)</i>
<i>Jiangxichelys ganzhouensis</i>	NHMG 010415, JXGZ(2012)-178, JXGZ(2012)-179, JXGZ(2012)-180, JXGZ(2012)-182	Ganzhou, Jiangxi	Late Cretaceous (Maastrichtian)	Lianhe Formation	<i>Tong & Mo (2010)</i> <i>Tong et al. (2016)</i>
<i>Yuchelys nanyangensis</i>	HGM NR09-11-14, CUGW EH051	Nanyang, Henan	Late Cretaceous (Turonian–middle Campanian)	Gaogou Formation	<i>Tong et al. (2012)</i> <i>Ke et al. (2021)</i>
Nanhsiungchelyidae indet.	Specimen number was unknown. The authors named it as 'Hefei specimen'	Jiangxi	Late Cretaceous	Unknown	<i>Hu et al. (2016)</i>

- 3 Note: this table does not include small fragments which has less taxonomic significance.
4

Table 2 (on next page)

Main differences among the three species of *Nanhsiungchelys*

1 Table 2:

2 Main differences among the three species of *Nanhsiungchelys*

Character	<i>Nanhsiungchelys yangi</i>	<i>N. wuchingensis</i>	<i>Nanhsiungchelys</i> sp. (SNHM 1558)
Snout	triangular (in dorsal view)	trumpet shaped	unknown
Premaxilla	higher than wide	wider than high in lateral view and has an inverse Y-shape in ventral view	unknown
Maxilla	unseen in dorsal views; a small portion of the maxilla extends posterior and ventral of the orbit	visible in dorsal views; the maxilla is located entirely anterior to the orbit	unknown
Jugal	higher than wide	wider than high	unknown
Prefrontal	convex dorsally behind the naris	concave behind the naris	unknown
Parietal	bigger than the frontal	smaller than the frontal	unknown
Mandible	the middle and posterior parts of the mandible are more robust than the most anterior part in ventral view	nearly all parts of the mandible are equal in width	unknown
Entoplastron	the angle between the two anterior edges of the entoplastron is wide (~110°)	the angle between the two anterior edges of the entoplastron is only ~100°	unknown
Anterolateral processes	wide	wide	slender

References	this paper	<i>Tong & Li (2019)</i>	<i>Hirayama et al. (2009)</i>
------------	------------	-----------------------------	-------------------------------

3